CDF Note 9097 Version 4.3
CDF/ANAL/EXOTIC/CDFR/9097
May 17, 2008

A Unified Search for the Supersymmetric Chargino-Neutralino Production at CDF in the Trilepton and Di-lepton + Track Channels with 2 fb^{-1}

Sourabh Dube, Julian Glatzer, Alex Sood, Sunil Somalwar

Abstract

CURRENT ANALYSIS STAGE: BLESSED
We describe a CDF II 2 fb^{-1} search for the Supersymmetric Chargino-Neutralino production through its R-parity conserving decays to three-lepton (lepton = e, μ) or di-lepton + clean track states. Allowing for the presence of a track in the signature makes this analysis sensitive to the τ leptonic decay modes of the Chargino-Neutralino parent state. A significant missing transverse energy is required in either case to account for the missing neutrinos and the Lightest Supersymmetric Particles (LSP's). This analysis unifies individual searches in several exclusive channels with varying signal/background ratios. The selection criteria in individual channels are adjusted to maximize the overall search sensitivity. Overall, we expect a total of 0.88 ± 0.09 background events for trilepton channels, and 5.5 ± 0.9 background events for dilepton+track channels with 2 fb^{-1} of data, expect to observe 4.5 ± 0.4, and 6.9 ± 0.6 signal events for a particular choice of mSUGRA model parameters respectively and we observe 1 events in the trilepton channel and 6 events in the dilepton+track channels. A limit is set on the cross section of Chargino-Neutralino pair production in a specific scenario.

This analysis differs from the previous CDFII 1 fb^{-1} Chargino-Neutralino search (documented in CDF8445[42] [14] and other notes, theses) in the following ways:
a) Our input is the combined high pt e and μ trigger datasets and the (overlapping) SUSY dilepton trigger dataset with overlaps removed.
b) Various analysis channels involving combinations of electrons, tight muons, CMIO muons, clean tracks etc are kept exclusive of each other and the selection criteria are chosen to maximize the

overall analysis sensitivity. In effect, an independent search is carried out in each channel and the results are combined.

Changes from v1.0 : We fixed the WW MC sample luminosity and also move to using the correct WZ MC sample. We also add a couple of clean-up cuts (such as $\Delta\Phi_{lep-\not\!\!E_T}$). We also add the expected limit plot.

Changes from v1.1 : We incorporate comments and suggestions made for v1.1. We also include descriptions of crosschecks such as splitting the control regions by lepton flavors. Minor fixes in code and minor changes to event selections are also included.

Changes from v2.0 : We include the background for dilepton+track channels where one of the leptons is a fake.

Changes from v2.1 : We include the details of the observed events in signal box in Section 12.

Changes from v3.0 : We include discussion on systematic errors for our signal and background predictions.

Changes from v3.1 : We include a section describing the SUSY parameter space for mSUGRA and our sensitivity in that space.

Changes from v4.1 : We update our exclusion plots with more MC points.

Changes from v4.2 : Slight update of some figures.

1 Introduction

1.1 Standard Model, SUSY, and $\widetilde{\chi}_1^{\pm}$-$\widetilde{\chi}_2^0$

The standard model (SM) has been a great achievement in particle physics. A large number of experimental results have confirmed many features of the theory to a high degree of precision. Nonetheless, the SM is theoretically incomplete in that it leaves many questions and problems [3, 4] unanswered. The most notable ones are the fine-tuning problem of the SM Higgs self-interaction through fermion loops [5] and the unknown origin of electroweak symmetry breaking (EWSB). Supersymmetry (SUSY) [6] incorporates an additional symmetry between fermions and bosons, and offers a solution to the fine-tuning problem and a possible mechanism for EWSB.

SUSY postulates that for each SM degree of freedom, there is a corresponding SUSY degree of freedom. This results in a large number of required supersymmetric particles (sparticles), and at least two Higgs doublets in the theory. A new quantum number, called R-parity (R_p) [8], is used to distinguish between SM particles and sparticles. All SM particles have $R_p = +1$ and sparticles have $R_p = -1$. The simplest extension to the SM, the minimal supersymmetric standard model (MSSM), respects the same $\mathrm{SU}(3) \otimes \mathrm{SU}(2) \otimes \mathrm{U}(1)$ gauge symmetries as does the SM. The analysis reported in this note focuses on searches in the framework of MSSM. Currently, the origin of SUSY breaking is still unknown. Various models of SUSY breaking have been postulated. Among them, Supergravity (SUGRA), in which gravity communicates the origins of SUSY breaking from a high mass scale to the electroweak scale, and Gauge mediated supersymmetry breaking (GMSB), in which a gauge interaction communicates the SUSY breaking between the two scales, are quite popular because of their relative simplicity.

Among SUGRA models, the so-called minimal SUGRA (mSUGRA [7]) model has been extensively studied. By assuming grand unification at a high mass scale ($\approx 10^{16}$ GeV), the MSSM spectrum (which in general has 124 free parameters) can be completely characterized by 4 parameters and a sign at the grand unification theory (GUT) scale [10]: a common scalar mass (m_0), a common gaugino mass ($m_{1/2}$), a common trilinear coupling value (A_0), the ratio of the vacuum expectation values of the two Higgs doublets ($\tan\beta$), and the sign of μ, where μ is the Higgsino mass parameter. Although it is desirable not to assume a specific SUSY breaking model (thus, a constraint) under MSSM in our searches, in order to have a sensible control of the parameters and to compare with other experiments, we conduct many of our searches along the line of mSUGRA model. A less constrained model, the cMSSM framework [11] is also considered. The parameters in cMSSM are: $\tan\beta$ and μ as defined above, and common gaugino mass at GUT scale (M_0), common sfermion mass at GUT scale (M_2), trilinear coupling in the stop sector (A_t), and the pseudoscaler neutral Higgs mass (M_A).

The golden search channel for mSUGRA is the $\widetilde{\chi}_2^0\widetilde{\chi}_1^{\pm} \rightarrow$ three leptons channel. It offers a reasonable signal $\sigma \times BR$ and there is very small contributions from Standard Model backgrounds.

1.2 Previous Results and Other Searches

Most of the current limits on MSSM are from the LEP2 experiments [12], from CDFII with 1 fb^{-1} data and from DZero. Most LEP searches have been presented in a process by process

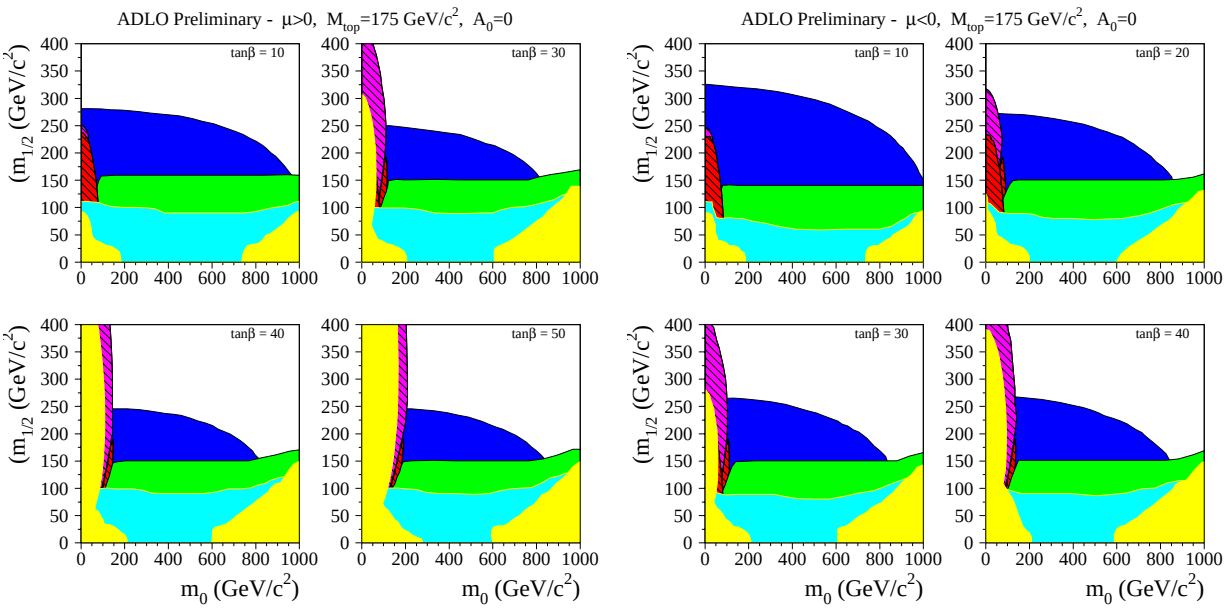

Figure 1: LEP2 Limit on mSUGRA for positive and negative μ, and for different $\tan\beta$. $A_0 = 0$ for all plots. ADLO refers to the four LEP experiments.Legend: Yellow -no mSUGRA solution, no EWSB or tachyonic particles, Light Blue -Regions inconsistent with measurements of EWK parameters at LEP1, Green -Regions excluded by chargino searches, Red -Regions excluded by selectron or stau standard searches, Blue -Regions excluded by search for hZ, Brown -Regions excluded by the neutralino stau cascade searches, Pink -Regions excluded by the search for heavy stable charged particles applied to staus.

fashion because the center of mass energy is well defined. We show here LEP2 limits for mSUGRA in the plane of m_0-$m_{1/2}$ in Figure 1. With $m_{top} = 175$ GeV and $A_0 = 0$, the limits on $M_{\widetilde{\chi}_0}$ is 59.0 GeV for $\mu > 0$ and 58.6 GeV for $\mu < 0$, respectively. The limit on $M_{\widetilde{\chi}_1^\pm}$ is 103.5 GeV.

The DZero collaboration also has published their results [15], but their results are only applicable for a fixed set of conditions.

1.3 Analysis Outline and Technical Details

In this note, we present an analysis that searches for $\widetilde{\chi}_2^0\widetilde{\chi}_1^\pm$ pair production decaying to three leptons (e,mu or tau) and invisibles in the mSUGRA model.

However, requiring that we always oberve three leptons as a signature is too restrictive. Since there is a substantial probability of producing a single charged hadron in the decay of a tau-lepton, allowing for the presence of a clean track along with two leptons increases sensitivity to tau leptons. We require that at least two of the three leptons to be electrons or muons. The last lepton can be an electron or muon or it can leave a track in the central tracker. This allows us to include one-prong tau leptons. Using the SUSY dilepton trigger dataset, we also try to reach as low in p_T-lepton as possible to expand our SUSY sensitivity.

We use an "unbiased" approach to the analysis: We define control regions to check our signal

and background estimation, optimize the cuts by comparing expected signal and background yields and only then look at the data in the signal region.

The backgrounds are Drell-Yan production (with a lepton from conversions, or a track from underlying event), diboson production and top pair production. Depending on the specific channel, the largest background is either WZ production, or Drell-Yan+track.

2 Data

The analysis is conducted in CDF offline releases 6.1 and Stntuple dev_243 is used as the main analysis ntuple.

We use the single lepton High P_T triggers, along with the SUSY Dilepton triggers. The High P_T triggers are fired by a single electron or muon with $P_T > 18$ GeV. Details about the High P_T triggers can be found in reference [41]. The SUSY Dilepton triggers require either two electrons or two muons with $P_T > 4$ GeV each. Details about the SUSY Dilepton triggers can be found in [42], [43]. The High P_T electron dataset has the identifier bhel, the High P_T muon dataset is bhmu and the SUSY Dilepton triggers are edil.

We use Good Run List version 18[16], with option (1,0,4,1)[1]. In summary, there are 3636 good runs. The total luminosity as calculated using the various scripts supplied by the Data Quality Management group is 2008 pb^{-1} for the High P_T electron triggers. This is corrected for the inelastic cross-section by a factor of 1.019.

The total luminosity is therefore 2046 pb^{-1}. This luminosity is then corrected for a $|Z_v| <$ 60 cm vertex cut [40] made to data. We use this luminosity as our standard luminosity and correct all other numbers (such as dynamic prescales to triggers) to this luminosity.

A part of data was processed in CDF software version 5.3 and amounts to about 362 pb^{-1}. The rest of the was data processed in version 6.1 and amounts to the remaining 1684 pb^{-1}.

A correction factor based on the Z_v distribution of DY MC is also applied to the luminosity of MC samples.

3 MC Samples

The Monte Carlo samples we for this analysis are listed in Table 1. The background samples we use are generated by the EWK group and the full details are listed elsewhere [44].

In the following text, signal point P1 refers to $m_0 = 60$ GeV, $m_{1/2} = 190$ GeV, $tan(\beta) = 3$, $\mu > 0$, and $A_0 = 0$. We show in Figure 2 the generator level p_T distributions for the three leptons, ordered in p_T for signal point P1. It is evident that we need to efficiently identify leptons with low p_T in order to maximize the sensitivity.

[1] We require the EM calorimeter and the muon system to be operating normally during data taking.

Sample	Xsec(pb)	MC Lum(fb^{-1})
Signal Point P1	0.472	217.8
DY, Z$\rightarrow ee$	355*1.4($\pm$3)	19.8
DY, Z$\rightarrow \mu\mu$	355*1.4($\pm$3)	20.3
DY, Z$\rightarrow \tau\tau$	355*1.4($\pm$3)	18.7
Z$\gamma \rightarrow ee\gamma$	10.33*1.36($\pm$3)	409
Z$\gamma \rightarrow \mu\mu\gamma$	10.33*1.36($\pm$3)	405
Z$\gamma \rightarrow \tau\tau\gamma$	10.33*1.36($\pm$3)	408
WW	1.27	404
WZ	0.208	559.6
ZZ	2.116	491.8
$t\bar{t}$	6.9	593.0

Table 1: Monte Carlo Samples. Cross section for the signal points is calculated using PROSPINO. The diboson backgrounds WW,ZZ and WZ include off-shell bosons. The background MC samples are generated by the EWK group.

4 Analysis Objects

The selection of leptons in this analysis is driven by the need to maximize acceptance while keeping the backgrounds down. We select electrons and divide them into two categories, 'tight' and 'loose'. The 'tight' electrons, henceforth called as TCE, are selected by imposing all the requirements in Table 2. The 'loose' electrons, henceforth called as LCE, are selected by imposing only the right part of the requirements in Table 2. Conversions are removed and a scale factor is applied to MC [45] to account for difference in conversion removal efficiency between data and MC.

The TCE are triggerable and have smaller backgrounds. The LCE, while being more efficiently selected, have higher backgrounds. See Section B for the fake rates for TCE and LCE.

We also select muons in three categories. The first two categories, CMUP and CMX are defined by the specific locations of the muons in our detector. The third muon category, CMIO muons, are stubless muons. The requirements on the selection of all three categories of muons are shown in Table 3. The CMUP and CMX muons can be thought of as the muon counterparts to the TCE, while CMIO is the muon counterpart to the LCE[2]. Thus a tight muon refers to the CMUP,CMX type muons and loose muon refers to the CMIO.

In terms of lepton identification, the MC represents data fairly well. However, there are

[2]The CMIO muon also differs from the CMUP,CMX muons in the sense that since it is stubless, it suffers from much larger backgrounds and fake rates (Section B).

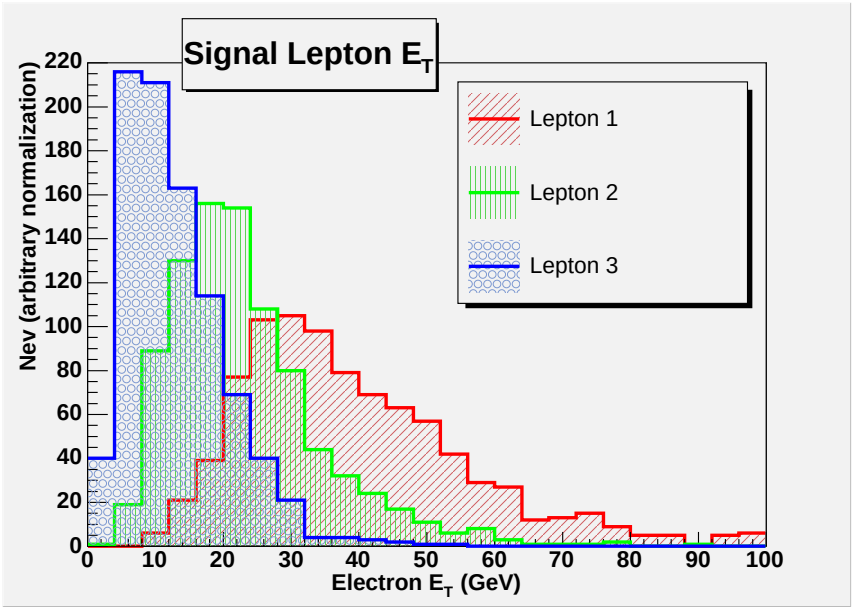

Figure 2: p_T distributions for generator level leptons for signal point A (see Table 1). Three lepton events are selected and the leptons are ordered in p_T.

Tight Electron Identification
CEM fiducial, Track $\lvert z_0\rvert < 60$ cm
$E_T \geq 5$ GeV, $P_T \geq 4$ GeV
Had/Em $< 0.055 + 0.00045 \times$ EmE/GeV
E/P < 2 if Track $p_T < 50$ GeV
Lshr < 0.2
-3 cm $<$ charge $\times \Delta X < 1.5$ cm
$\lvert\Delta Z\rvert < 3$ cm
CES $\chi^2_{\rm strip} < 10$
NAxialSeg(5) ≥ 3, NStereoSeg(5) ≥ 2
if $E_T > 20$, fractional isolation < 0.1
if $E_T < 20$, isolation energy < 2 GeV

Loose Electron Identification
CEM fiducial, Track $\lvert z_0\rvert < 60$ cm
$E_T \geq 5$ GeV, $P_T \geq 4$ GeV
Had/Em $< 0.055 + 0.00045 \times$ EmE/GeV
NAxialSeg(5) ≥ 3, NStereoSeg(5) ≥ 2
CES $\chi^2_{\rm strip} < 20$
fractional isolation < 0.1

Table 2: Electron Identification Cuts, left for TCE, right for LCE.

ID Cut	CMUP,CMX	CMIO
$\|\eta\|$	≤ 1.0	≤ 1.0
BCP_T GeV	≥ 5	≥ 10
$Track\|z_0\|$ cm	≤ 60	≤ 60
Fiduciality	(CMU & CMP) or CMX	Not CMUP, Not CMX
Stub Matching CMU,CMP,CMX cm	$\Delta X \leq 7, 5, 6$	-
Track χ^2 (Data)	≤ 2.3	≤ 2.3
Corrected d_0 cm	$\leq 0.2(0.02)$ Si Hits (no Si Hits)	$\leq 0.2(0.02)$ Si Hits (no Si Hits)
NAxialSeg(5)/NStereoSeg(5)	$\geq 3/2$	$\geq 3/3$
Hadronic Energy GeV	≤ 6+sliding	≤ 6+sliding
EM Energy GeV	≤ 2 +sliding	≤ 2 +sliding
EM+Had Energy	≥ 0.1 GeV	≥ 0.1 GeV
fractional isolation	≤ 0.1	≤ 0.1

Table 3: Muon Identification Cuts.

differences and these are dealt with by measuring scale factors (E_T dependent). These scalefactors are then applied to MC on an event by event basis. The electron and muon scale factors are summarized in Table 4. We take the track identification scale factor to be 1.0. The scale factors are obtained mainly from [41]. The different scale factors for various data taking periods are combined with the correct luminosity weights and we use a single number for each category for the whole analysis.

In addition to using electrons and muons, we also wish to be senstive to the hadronic decay of tau leptons. It is interesting to note that the single-prong decays of the tau cover 85% of its decays, of which 50% are non-leptonic. In the single-prong decay, the tau decays to one charged particle only (with accompanying neutrinos). By selecting single isolated tracks in addition to the electrons and muons, we can be sensitive to most of the tau decays. We select tracks passing requirements listed in Table 5. In terms of signal acceptance, the tracks are significant in increasing our acceptance. Of course, the acceptance of background also increases, but this can be dealt with by imposing selections to reduce background if there is a track in the event (see Section 10).

5 Exclusive Channels

Once we have selected our analysis objects, we then proceed to select exclusive analysis channels. The channels are selected based on the quality of the lepton objects. Table 6 gives the details of the channels. Table 7 gives the channels for dilepton events. Of course,each channel can be

Lepton	E_T **range**	**Scale factor**
TCE	≥ 20 GeV	0.98(0.006)
TCE	8 - 20 GeV	0.96(0.02)
TCE	5 - 8 GeV	0.88(0.16)
LCE	≥ 20 GeV	0.96(0.03)
LCE	8 - 20 GeV	0.97(0.03)
CMUP	≥ 20 GeV	0.94(0.006)
CMUP	5 - 20 GeV	0.87(0.04)
CMX	≥ 20 GeV	0.99(0.01)
CMX	5 - 20 GeV	0.88(0.04)
CMIO	≥ 20 GeV	1.0(0.01)
CMIO	10 - 20 GeV	1.0(0.06)

Table 4: Lepton identification scale factors used in this analysis.

$p_T > 5$ GeV
$\|z_0\| < 60$ cm
Number of COT stereo segments with at least 5 hits ≥ 3
Number of COT axial segments with at least 5 hits ≥ 3
fractional track isolation $= 0$ [24]

Table 5: Isolated track requirements.

further split depending on the lepton flavors for testing purposes.

6 Preliminary Selections

The highest p_T vertex with CDF Quality 12 is chosen to be the event vertex. In addition to our primary analysis objects, we select jets if they satisfy the following criteria: raw $E_T > 8$ GeV, level-5 corrected $E_T > 15$ GeV and EM fraction < 0.9.

We then correct the $\not\!\!E_T$ for jets and the selected muons. Details regarding these corrections can be found in [42], [38]. We also correct the $\not\!\!E_T$ for isolated tracks for the dilepton+trk channels.

We require that the $\Delta R_{\eta-\phi}$ separation be above 0.4 between lepton-pairs, lepton-track, lepton-jet and track-jet.

Channel Name	**Selection**	$(E_T/P_T)_{1,2,3}GeV$
ttt	3 tight leptons or 2 tight leptons + 1 loose electron	15, 5, 5
ttC	2 tight leptons + 1 CMIO	15,5,10
tll	1 tight leptons + 2 loose leptons	20, 8, 5(10 if CMIO)
ttT_τ	2 tight leptons + 1 isolated track	15, 5, 5
tlT_τ	1 tight + 1 loose lepton + 1 isolated track	20, 8(10 if CMIO), 5

Table 6: The exclusive analysis channels.

Channel Name	**Selection**	$(E_T/P_T)_{1,2}GeV$
tt	2 tight leptons	15, 5
tl	1 tight lepton + 1 loose lepton	20, 8(10 if CMIO)

Table 7: The exclusive analysis channels.

Jet energy mismeasurement might lead to false $\not\!\!E_T$ in our events. Since our signal selection requires $\not\!\!E_T$, we decide to cut away such events with false $\not\!\!E_T$. Based on studies for previous versions of this analysis [42], we reject any events where the $\not\!\!E_T$ and any jet ($E_T > 10$GeV) are azimuthally separated by less than 0.35 radians.

To further remove backgrounds from mismeasured $\not\!\!E_T$, we ask that the azimuthal separation between leading lepton and $\not\!\!E_T$ and that between next-to-leading lepton and $\not\!\!E_T$ be more than 0.17 rad. Figure 3 shows the distributions of azimuthal separation between leptons and $\not\!\!E_T$ for signal and for Drell Yan events (DY has no intrinsic $\not\!\!E_T$). As seen from the figure, these selections are fairly loose for signal.

We also require that the lepton pair mass for dilepton selection is above 20 GeV/c^2. This is to remove any J/ψ, Υ contributions, and since our Drell-Yan MC has a generator level cut at 20 GeV/c^2. For the trilepton (dilepton+track) selection there are two opposite-sign lepton pairs. The higher of the two OS pair masses is used to define the control regions. The higher of the two OS pair masses is required to be above 20 GeV/c^2, the next highest OS pair mass is required to be above 13 GeV/c^2 for all trilepton (dilepton+track) events.

Since the third lepton goes fairly low in P_T, we require that the it is tightly isolated. We do this by requiring the fractional isolation less than 0.1, and the track isolation [24] less than 0.1. For dilepton+track events, the softer leptons is also required to be tight track isolated. We also require that aside from the three primary objects (Table 6), there is no other analysis level object above 10 GeV in the event.

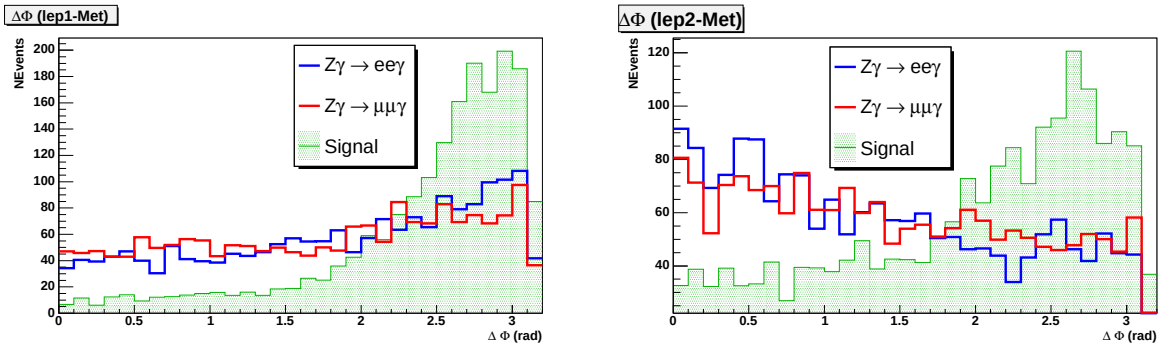

Figure 3: Signal and DY distributions for angle between leading lepton and $\not\!\!E_T$ on left and next-to-leading lepton and $\not\!\!E_T$ on right . The distributions are normalized to area.

7 Trigger Efficiencies

The trigger efficiencies for the High P_T datasets is described in [41]. The di-electron paths of the SUSY dilepton dataset is described in [42], while the di-muon paths are described in [46].

The High P_T muon triggers require special consideration. The trigger paths for this dataset have changed considerably over the data taking period. The authors are thankful for the efficiency measurements [41] which are available and are corrected for issues such as dynamic prescaling. However, since the triggers are not all present all the time, it remains upto us to account for the presence of various paths at different periods in the data.

Using the unchanged High P_T electron triggers to obtain a benchmark luminosity, we then weight the efficiencies of the various muon paths by the amount of time they were present in the data taking period.

Thus for example, if path A was present in the data for only 500 pb^{-1}, then the efficiency of path A (ϵ_A) is taken to be

$$\epsilon_A^{corr} = \epsilon_A \times \frac{500}{2000}$$

where 2000 pb^{-1} is the total amount of data we are analysing. In such a way the corrected efficiencies for all the various paths of the High P_T muon dataset are obtained.

The SUSY dilepton trigger paths have different thresholds for the last 191 pb^{-1} of data. The thresholds change from 4,4 GeV for both leptons, to 8,4 GeV. We have verified that the trigger is fully efficient for the thresholds we have for our channels(Table 6) and thus there is no effect of the change in thresholds of the SUSY triggers.

8 Estimating Backgrounds

To estimated backgrounds, we use the methods developed and described in previous trilepton analyses [42] [38] [39]. We include a brief desciption here.

8.1 Trilepton Channels

Background processes which give three genuine leptons (WZ/γ^*,ZZ,$t\bar{t}$) are estimated from MC. All trilepton events passing final selections (for signal box) or specific kinematic selections (for control regions) are weighted by trigger efficiencies and lepton identification scalefactors and the respective event weights are summed. Background processes with two leptons (dominated by Drell Yan) where the third lepton comes from conversion of a radiated photon are also estimated from the MC. Thus the Drell Yan contributions to the trilepton channels are estimated by using the Drell-Yan MC and requiring that one of the primary leptons from the DY process radiates a photon.

The remaining background is where two real leptons are accompanied by a third lepton from underlying event. This contribution is called 'fake' contribution. The fake rates (See Appendix B) are measured in jet-triggered data. To estimate the fake contribution (in signal or control regions) we select events with two well identified leptons and one fakeable object. The fakeable object for electrons is a jet of certain quality and for muons is a track of some quality. The fake rate corresponding the fakeable object is then applied to this event as a weight, and the fakeable object is then treated as a real lepton. The event is taken through all the selections and the sum of weights of all such events is the total fake contribution. It is worth noting that we ignore the contributions from events with one real lepton and two fake leptons. Such 'double-fake' contribution is taken to be negligible[39].

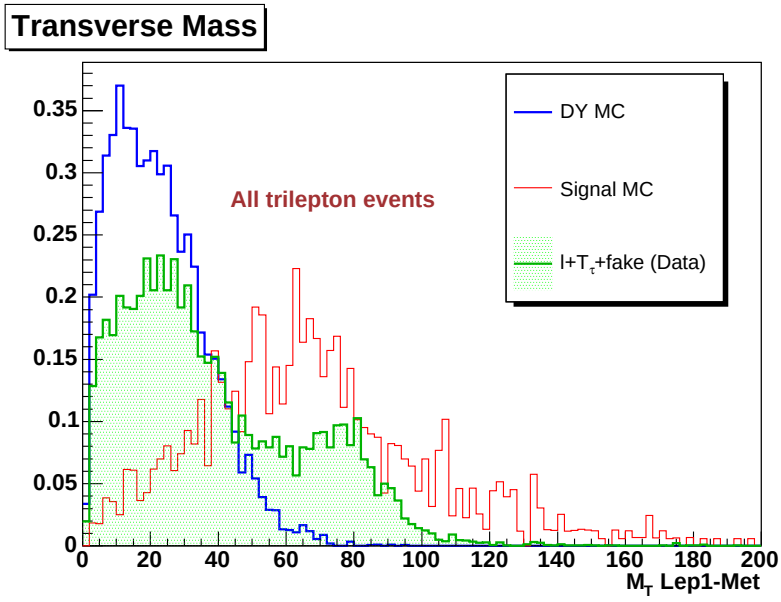

Figure 4: We show the transverse mass distribution of leading lepton with $\not\!\!E_T$ for all ttT_τ events with the 'fake' lepton background in green (l+T_τ+fake). For reference, the DY and signal MC is also shown. More details are in the text.

8.2 Dilepton+Track Channels

The backgrounds to the dilepton+track channels can be split into three contributions -

- The backgrounds that come from three real leptons (WZ/γ^*,ZZ) are estimated from the MC samples as for the trilepton channels.
- The backgrounds with two real leptons and an isolated track from the underlying event are estimated using the isolated track rate method (See Appendix A). The track rate is measured in the Z data sample as a function of the number of tracks in the event. It is then applied to the MC samples. The track kinematics are obtained from MC events with real identified tracks. The exact procedure is described in detail in the appendix.
- The backgrounds with one real lepton and one isolated track with a third lepton from underlying event. This contribution has two parts :
  - Drell-Yan process where one lepton fails lepton selection and is reconstructed as isolated track plus an additional lepton from underlying event.
  - W + jet events giving one real lepton (from W), one isolated track, and one lepton from underlying event.

  We can estimate both of these contributions together by estimating the 'fake' contribution as for trilepton channels. Specifically, we select one lepton + isolated track events. We then select a fakeable object and apply the fake rate for leptons in the same way as the trilepton channels.. The sum of weights gives us the contribution to dilepton+track events where one lepton comes from underlying event. Figure 4 shows the transverse mass distribution for the identified lepton with $\not\!\!E_T$ for this background. For reference, the same distributions in DY and signal MC are also shown. The contributions from Drell-Yan and W+jets are identifiable in the l+T_τ+fake distribution.

9 Control Regions

We devise several control regions to verify our background estimations. The various control regions are illustrated in Fig 5. We split our sample into different regions based on $\not\!\!E_T$ and Invariant Mass of two leptons.

These regions are further split into dilepton and trilepton regions - only two leptons are required for the dilepton regions, an additional lepton or track is required for the trilepton regions.

The dilepton control regions are further split into ones with 2 tight leptons and ones with 1 tight + 1 loose lepton. The trilepton control regions are divided into the channels described in Section 5.

The summary plots of the dilepton and trilepton control regions are shown in Figures 7 and 6. We describe a few control regions here. The appendices contain more numbers and distributions for the control regions.

We start with the trilepton control regions :

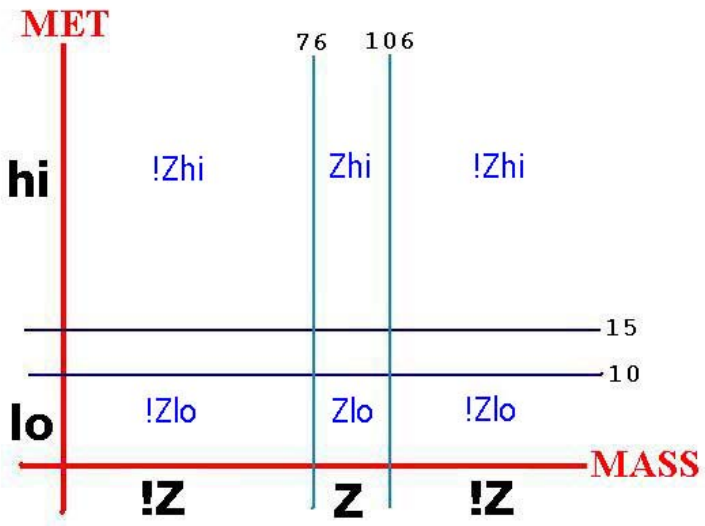

Figure 5: Illustration of the various control regions considered. See text for details

9.1 Trilepton Control Region "!Zlo": $M^1_{os} < 76$ or $M^1_{os} > 106$, $\not\!\!E_T \leq 10$

We select this control region with the following requirements:

- $\not\!\!E_T < 10$ GeV
- The maximum OS mass should not be in the Z mass window (76 to 106 GeV/c^2).
- Correct charge combination of trileptons: $|\sum charge| = 1$.

The expected number of SM and signal events and observed number of events are listed in Table 8.

9.2 Trilepton Control Region "Zlo": $76 < M^1_{os} < 106$, $\not\!\!E_T \leq 10$

We select this control region with the following requirements:

- $\not\!\!E_T < 10$ GeV
- The maximum OS mass should be in the Z mass window (76 to 106 GeV/c^2).
- Correct charge combination of trileptons: $|\sum charge| = 1$.

The expected number of SM and signal events and observed number of events are listed in Table 9.

Channel	Predicted Background	Observed
ttt	6.3 ± 2.7	9
ttC	2.2 ± 1.5	3
tll	1.4 ± 1.3	0
Combined trilepton	10.9 ± 3.3	12
ttT_τ	88 ± 13	72
tlT_τ	34 ± 7	31

Table 8: Expected number of background events and observed number of events in data in Control Region !Zlo. Uncertainty includes contributions from MC statistics and partial systematics (fake rate, lepton ID and trigger efficiencies).

Channel	Predicted Background	Observed
ttt	10.8 ± 4.2	8
ttC	4.9 ± 2.5	6
tll	2.8 ± 1.9	3
Combined trilepton	18.5 ± 5.2	17
ttT_τ	223 ± 26	218
tlT_τ	195 ± 26	183

Table 9: Expected number of background events and observed number of events in data in Control Region Zlo. Uncertainty includes contributions from MC statistics and partial systematics (fake rate, lepton ID and trigger efficiencies).

9.3 Trilepton Control Region "Zhi": $76 < M^1_{os} < 106$, $\not\!\!E_T \geq 15$

We select this control region with the following requirements:

- $\not\!\!E_T > 15$ GeV
- The maximum OS mass should be in the Z mass window (76 to 106 GeV/c^2).
- Correct charge combination of trileptons: $|\sum charge| = 1$.

The expected number of SM and signal events and observed number of events are listed in Table 10.

We now describe a couple of the dilepton regions :

Channel	Predicted Background	Observed
ttt	2.7 ± 1.7	0
ttC	1.7 ± 1.3	2
tll	1.6 ± 1.3	2
Combined trilepton	6.0 ± 2.5	4
ttT_τ	26.8 ± 6.0	34
tlT_τ	27.7 ± 6.3	23

Table 10: Expected number of background events and observed number of events in data in Control Region Zhi. Uncertainty includes contributions from MC statistics and partial systematics (fake rate, lepton ID and trigger efficiencies).

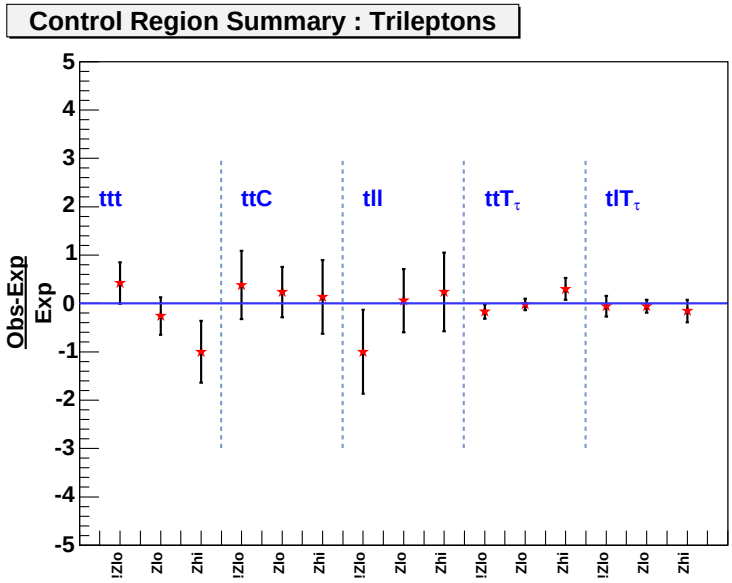

Figure 6: Overall comparison of the various trilepton control regions we study. Errors include statistical and partial systematics.

9.4 Dilepton Control Region "Z": $76 < M_{ll} < 106$,

We select this control region with the following requirements:

- The lepton pair mass should be in the Z mass window (76 to 106 GeV/c^2).

The expected number of SM and signal events and observed number of events are listed in Table 11.

Channel	Predicted Background	Observed
tt	51150 ± 2034	51042
Z→ee	31222 ± 1710	31074
Z→ $\mu\mu$	19895 ± 1102	19942
tl	42288 ± 1868	41833
Z→ee	10591 ± 664	10235
Z→ $\mu\mu$	30947 ± 1728	30958
Combined dilepton	93438 ± 2762	92875

Table 11: Expected number of background events and observed number of events in data in Control Region Z. Uncertainty includes contributions from MC statistics and partial systematics (lepton ID and trigger efficiencies and DY crosssection uncertainty).

9.5 Dilepton Control Region "!Z": $M_{ll} < 76$ or $M_{ll} > 106$

We select this control region with the following requirements:

- The lepton pair mass should not be in the Z mass window (76 to 106 GeV/c^2).
- The lepton pair mass should be greater than 20 GeV/c^2.

The expected number of SM and signal events and observed number of events are listed in Table 12.

Channel	Predicted Background	Observed
tt	16352 ± 716	15966
!Z→ee	10399 ± 617	10033
!Z→ $\mu\mu$	5290 ± 352	5198
tl	7198 ± 300	7069
!Z→ee	1855 ± 114	1890
!Z→ $\mu\mu$	4550 ± 261	4482
Combined dilepton	23550 ± 776	23035

Table 12: Expected number of background events and observed number of events in data in Control Region !Z. Uncertainty includes contributions from MC statistics and partial systematics (lepton ID and trigger efficiencies and DY crosssection uncertainty).

9.6 Summary of the Control Region Studies

After examing all control regions, we conclude that our background estimation and observation are in good agreement. See Appendix C for tables of the control regions for all regions and all categories.

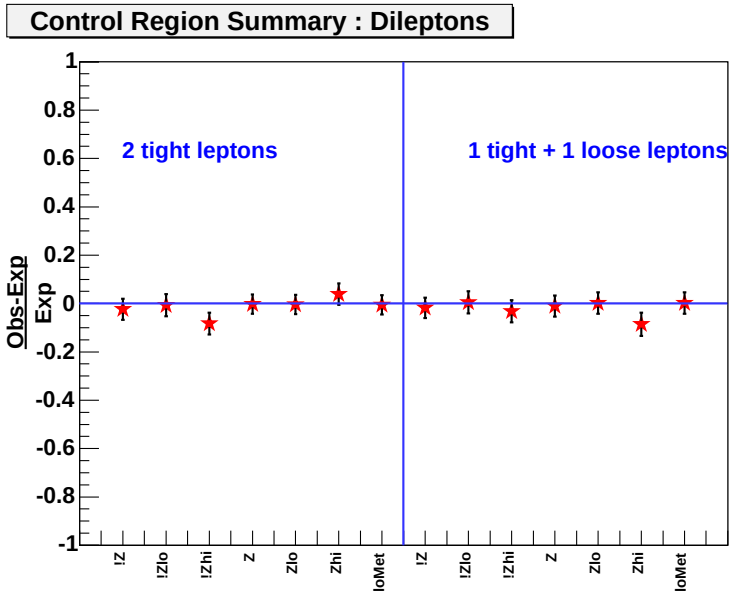

Figure 7: Overall comparison of the various dilepton control regions we study. Errors include statistical and partial systematics.

10 Optimized Selection for SUSY Signal

10.1 Nominal optimized selection cuts for SUSY signal

In addition to the pre-selection described in section 5 and section 6 , we require that the events must have correct charge combination, i.e., $|\sum leptoncharge| = 1$. We then decide the final cuts to enrich the SUSY signal by performing a (N-1) optimization. Since the parameter space for signal is large and this optimization is done for only a single signal point, we use the results of the scan only to guide our eye and pick the final cuts conservatively to retain signal. The final cuts are listed in Table 13. Our selections are mainly motivated by the studies done for the previous round of this analysis [42],[43],[38],[39].

Here is a description of each of the optimization cuts :

- $\not\!\!E_T \geq 20$ GeV : We require the missing E_T in the event to be above 20 GeV. This cut reduces the Drell Yan background, which has intrinsically low $\not\!\!E_T$.

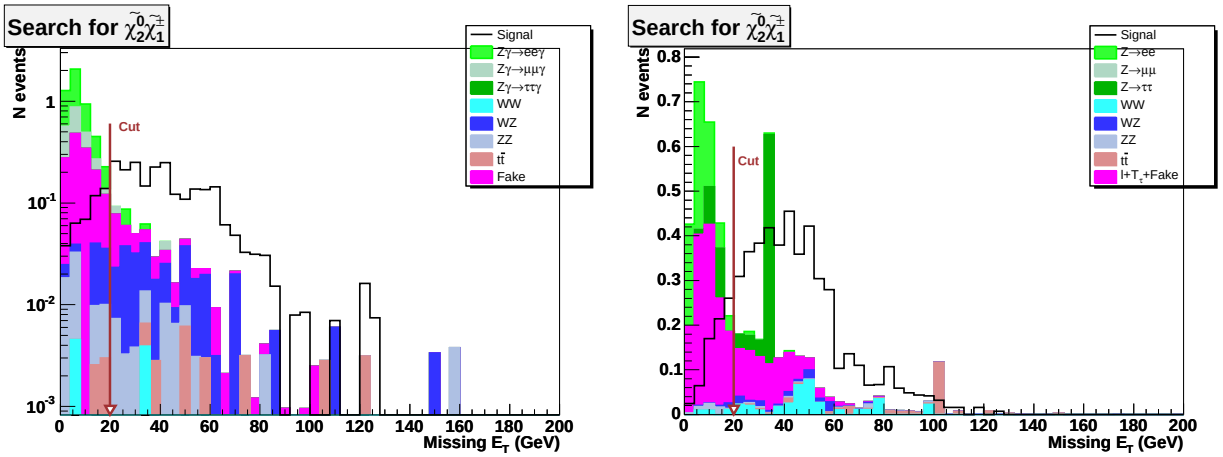

Figure 8: Signal and background $\not\!\!E_T$ distributions **ttt** on left and **tt**T_τ on right. Background histograms are stacked. Signal distribution is shown in black open histogram. All samples are normalized to the data luminosity. We select events with $\not\!\!E_T > 20$ GeV. For the plot all cuts listed in Table 13 except $\not\!\!E_T$ are applied.

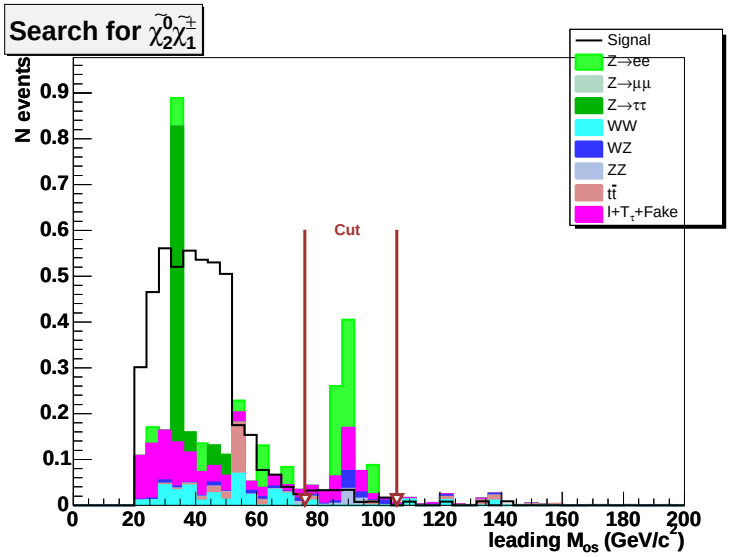

Figure 9: Signal and background maximum opposite sign mass distribution for **tt**T_τ. Background histograms are stacked. Signal distribution is shown in black open histogram. All samples are normalized to the data luminosity. We reject events with mass in the Z-mass window, viz. 76 to 106 GeV/c^2. For the plot, all cuts listed in Table 13 except veto on this mass are applied.

- $\Delta\phi_{os} \leq 2.9(2.8)$ rad : In addition to $\not\!\!E_T$, we can further reduce Drell Yan background by requiring that any opposite charged lepton (or lepton-track) pairs are not back-to-back.

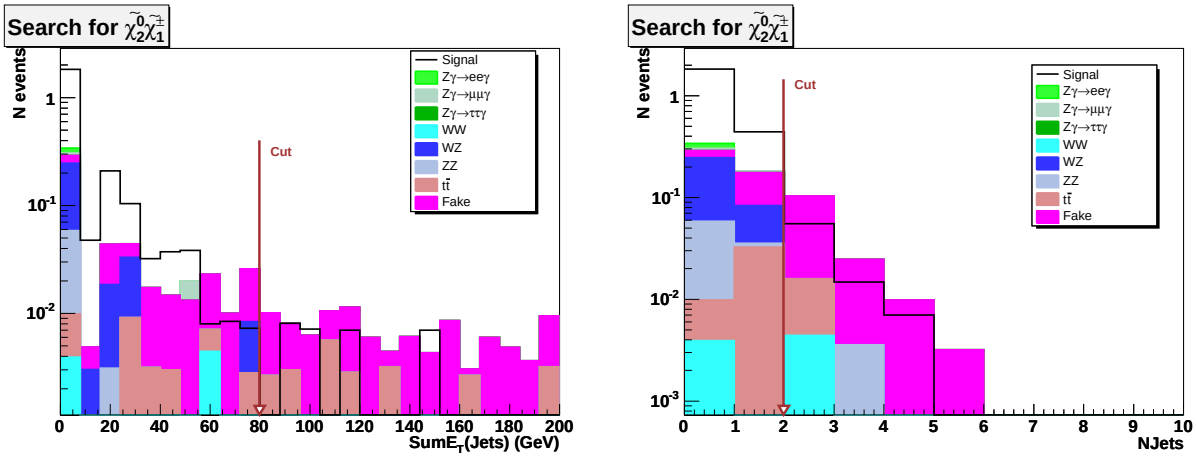

Figure 10: Signal and background SumE_T of jets distribution on left and number of Jets on right for **ttt** . Background histograms are stacked. Signal distribution is shown in black open histogram. All samples are normalized to the data luminosity. We select events with SumE_T < 80 GeV and Njets < 2. For the plots, all cuts listed in Table 13 except SumE_T and Njets are applied

The cut is tightened from 2.9 to 2.8 for the dilepton+track channels since the Drell Yan background is larger for those channels.

- Vetoes on Z mass : To remove potential Z events, we require that none of the opposite charged lepton (or lepton-track) pairs form a mass in the Z window ($76 \leq M_{ll} GeV/c^2 \leq 106$.

- Sum$E_T \leq$ 80 GeV : We take the total sum of E_T of all jets ($E_T^{corr} \geq 15 GeV$) in our event and require this sum to be less than 80 GeV. This is done to reduce the $t\bar{t}$ background. Moreover, our signal topology has no hard jets.

- Njets < 2 : We require that there is no more than one jet ($E_T^{corr} \geq 15 GeV$). This requirement along with the SumE_T requirement will remove any background from $t\bar{t}$ and residual QCD background.

Figures 8, 9, 10, 11, show the distributions for one optimization variable after some other selections are made. After the optimized cuts, the number of expected background and signal events are listed in Table 14. Overall, we expect a total of 0.88 ± 0.08 background events for trilepton channels, and 5.5 ± 0.8 background events for dilepton+track channels with 2fb^{-1} of data, expect to observe 4.5 ± 0.3, and 6.9 ± 0.3 signal events, respectively.

11 Systematic Errors

The systematic errors we consider follow from previous trilepton analyses [42],[39],[38]. The sources of systematic errors and their magnitude is listed in Table 15 (See Appendix D for a full breakdown). The systematic errors are

Variable	Trilepton	Dilepton+Track
$\not\!\!E_T$	> 20 GeV	> 20 GeV
$\Delta\phi_{os}$	< 2.9 rad	< 2.8 rad
max OS Mass	Z veto	Z veto
next OS Mass	Z veto	Z veto
SumE_T	< 80 GeV	< 80 GeV
Njets	< 2	< 2

Table 13: Final selection cuts. Description for each cut can be found in text.

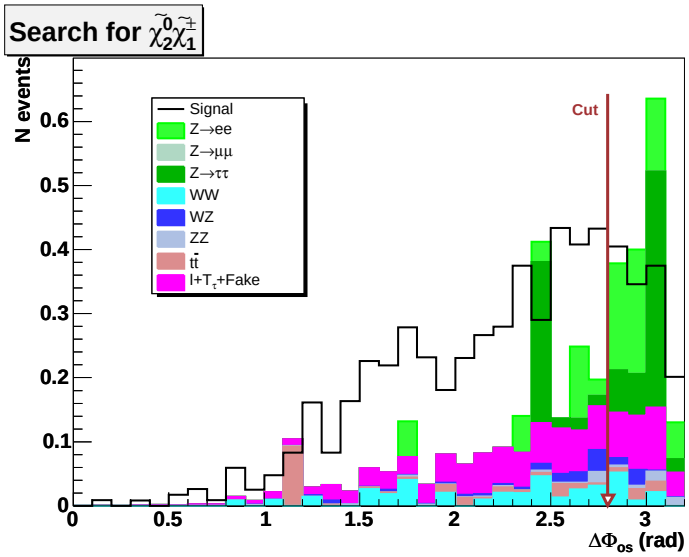

Figure 11: Signal and background $\Delta\phi_{12}$ distribution for $\mathbf{tt}T_\tau$. Background histograms are stacked. Signal distribution is shown in black open histogram. All samples are normalized to the data luminosity. We select events with $\Delta\phi_{12} < 2.8$ rad. For the plot, all cuts listed in Table 13 except $\Delta\phi_{12}$ are applied.

- ID : The errors on the lepton identification scalefactors as described in their respective measurements.
- Trig : The errors on the trigger efficiencies as described in their respective measurements.
- JES : For the jet energy scale (JES) we fluctuate the jet energies by 1σ up and down according to the standard prescription and evaluate the difference of acceptance from the nominal. In case the statistics preclude such an estimation, we take the difference from nominal for a

Box	Z→ee	Z→ $\mu\mu$	Z→ $\tau\tau$	WW	WZ/γ^*	ZZ	tt	fake	Background	Signal P1
ttt	0.03	0.02	0.00	0.00	0.24	0.05	0.02	0.12	0.49 ± 0.07	2.25 ± 0.17
ttC	0.00	0.01	0.00	0.00	0.13	0.07	0.01	0.04	0.25 ± 0.03	1.61 ± 0.13
tll	0.00	0.00	0.00	0.00	0.06	0.02	0.03	0.03	0.14 ± 0.02	0.68 ± 0.08
ttT_τ	0.81	0.00	0.82	0.38	0.15	0.08	0.22	0.75	3.22 ± 0.60	4.44 ± 0.22
tlT_τ	0.73	0.30	0.29	0.29	0.05	0.04	0.18	0.41	2.28 ± 0.51	2.42 ± 0.16

Table 14: Number of expected signal and background events in 2 fb^{-1} of data. Uncertainties are statistical and partial systematics. The fake numbers for trilepton channels are for 2 leptons + a fake lepton. For the dilepton+track channels the fake numbers are for 1 lepton + 1 T_τ + fake lepton.

'signal' like selection, viz. two leptons with $\not\!\!E_T$ >20 GeV, SumE_T(Jets)<80 GeV, Njets <2, $\Delta\phi_{12} < 2.9$ radians.

- X-sec : The error on the cross section of the background process. We use the errors quoted by the CDF WZ search [48] for dibosons, and the top mass measurement([49]) for the $t\bar{t}$ cross section.
- PDF : For the PDF uncertainties, we use the numbers quoted by the CDF WZ search, and the top mass measurement.
- ISR/FSR : The effects of turning on the initial state(ISR) and final state(FSR) radiation have been studied for previous rounds, and we use those measurements here.
- Conv : The systematic error on the conversion scale factor is taken from the measurement of the scalefactor([45]). This is applied to the backgrounds for the trilepton channels, where we expect the third lepton to have come from a photon conversion such as Z$\gamma \rightarrow ee\gamma$.
- ITR(nom) : This systematic is applied to the dilepton+track channels. It is the error on the isolated track rate measurement as described in appendix A.
- ITR(alt) : We also use an alternate parametrization for the isolated track rate. We parametrize the track rate as a function of the SumE_T of all jets ($E_T^{corr} > 10$) in the event. We take the difference from the nominal estimate as the systematic error.
- Fake : This is the error on the fake lepton measurement which we take to be 50%. The measurement method is described in detail in [47].

We also perform a systematic check for the $\not\!\!E_T$ correction for tracks in our event. For the tracks, we make no assumption about the type of charged particle giving the track. We correct the $\not\!\!E_T$ for the track if the $E_T/p_T \leq 1$ for the track. To test if this selection has any systematic effect,

we change this selection to $E_T/p_T \leq 0.8$ and check the deviation from nominal. We find that there is no significant deviation, and this selection is not a source of systematic error.

Channel/Source	ID	Trig	JES	X-sec	PDF	ISR/FSR	Conv	ITR(nom)	ITR(alt)	Fake
ttt	2.3	0.3	1.5	5.0	1.4	2.3	2.2	-	-	12.2
ttC	2.5	0.3	1.7	5.9	1.6	2.5	2.1	-	-	8
tll	2.2	0.3	3.5	5.0	1.3	2.2	1.8	-	-	10.7
ttT_τ	1.8	0.2	3.9	2.3	1.5	1.8	-	5.8	6.0	11.6
tlT_τ	1.8	0.2	5.2	2.4	1.5	1.8	-	8.6	10.5	9.0
Signal	4	0.5	0.5	10	2	4	-	-	-	-

Table 15: The systematic errors for the different channels broken down by source in percentage. A universal 6% uncertainty on the luminosity is not included in this table.

Channel	Background	Signal	Observed
ttt	$0.49 \pm 0.04(\mathrm{stat}) \pm 0.07(\mathrm{syst})$	$2.25 \pm 0.13(\mathrm{stat}) \pm 0.26(\mathrm{syst})$	1
ttC	$0.25 \pm 0.03(\mathrm{stat}) \pm 0.03(\mathrm{syst})$	$1.61 \pm 0.11(\mathrm{stat}) \pm 0.19(\mathrm{syst})$	0
tll	$0.14 \pm 0.02(\mathrm{stat}) \pm 0.02(\mathrm{syst})$	$0.68 \pm 0.07(\mathrm{stat}) \pm 0.08(\mathrm{syst})$	0
Trilepton	$0.88 \pm 0.05(\mathrm{stat}) \pm 0.08(\mathrm{syst})$	$4.5 \pm 0.2(\mathrm{stat}) \pm 0.3(\mathrm{syst})$	1
$\mathbf{ttT}_\tau$	$3.22 \pm 0.48(\mathrm{stat}) \pm 0.49(\mathrm{syst})$	$4.44 \pm 0.19(\mathrm{stat}) \pm 0.52(\mathrm{syst})$	4
$\mathbf{tlT}_\tau$	$2.28 \pm 0.47(\mathrm{stat}) \pm 0.40(\mathrm{syst})$	$2.42 \pm 0.14(\mathrm{stat}) \pm 0.28(\mathrm{syst})$	2
Dilepton+Track	$5.5 \pm 0.7(\mathrm{stat}) \pm 0.6(\mathrm{syst})$	$6.9 \pm 0.2(\mathrm{stat}) \pm 0.6(\mathrm{syst})$	6

Table 16: Number of expected signal and background events and number of observed events in 2 fb^{-1}. Uncertainties are statistical(stat) and full systematics(syst).

12 Result

Table 14 shows the expected number of background and signal events in each channel. After we open the signal box, we find 1 event in the ttt channel, 4 events in the ttT_τ channel and 2 events in the tlT_τ channel. Table 16 shows the expected SM background, signal and observed events.

Figure 12 shows the expected and observed limits for the mSUGRA model, in the region dominated by two-body decays of the $\widetilde{\chi}_1^\pm$ and the $\widetilde{\chi}_2^0$. We exclude chargino masses below approximately 145 GeV/c^2 in the mSUGRA model with parameters fixed as indicated in the figure.

Figure 13 shows the expected and observed limits for the mSUGRA model in the region dominated by three-body decays of the $\widetilde{\chi}_1^{\pm}$, and the $\widetilde{\chi}_2^0$. Here we vary $m_{1/2}$ to obtain the chargino mass while keeping $m_0 = 100$. At chargino mass of 130 Gev/c^2 we cross into the region where slepton is lighter than the chargino. The neutralino decay via the sleptons ($\widetilde{\chi}_2^0 \rightarrow \tilde{l}^{\pm} l^{\mp}$) gives a soft lepton below the thresholds of our analysis. The acceptance, and thus the limits worsen. The improve once again after the lepton moves over our threshold. We exclude chargino masses below approximately 127 GeV/c^2 in this case.

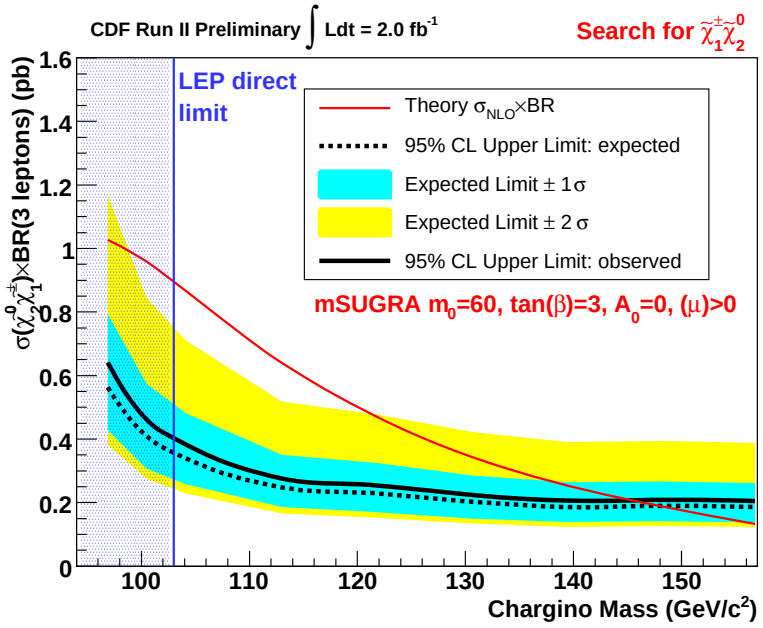

Figure 12: We show the expected and observed limits for the mSUGRA model. The red curve shows the theory cross-section×branching ratio. The black dashed curve shows the expected limit from this analysis with the 1 σ error on the expected limit in cyan and 2 σ in yellow. The solid black curve shows the observed limit. We exclude chargino masses below approximately 145 GeV/c^2 in this specific model.

13 Examination of Observed Events

In Table 17 we show some characteristics of the observed events. The event displays are linked from the analysis webpage [50].

14 Exploring mSUGRA parameter space

There are various supersymmetric models that may be used as guidelines for an analysis to search for signs of supersymmetry (SUSY). The analysis we have performed here is the search

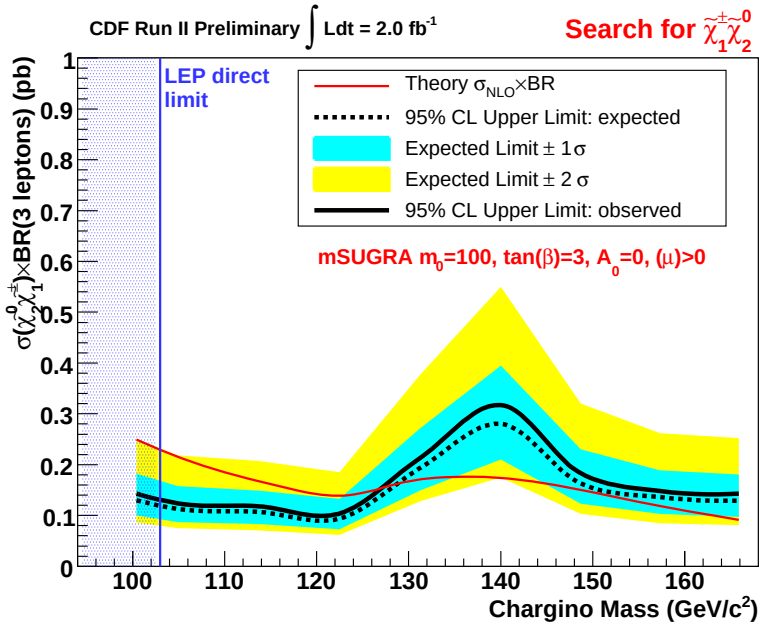

Figure 13: We show the expected and observed limits for the mSUGRA model. The red curve shows the theory cross-section×branching ratio. The black dashed curve shows the expected limit from this analysis with the 1 σ error on the expected limit in cyan and 2 σ in yellow. The solid black curve shows the observed limit. We exclude chargino masses below approximately 127 GeV/c^2 in this specific model.

Channel	Run	Event	Type	E_T^1	E_T^2	E_T^3	M_{OS}^1	M_{OS}^2	MET	Jet^1E_T
ttt	197716	2528577	-TCE +TCE -TCE	23.6	17.2	5.8	29.1	15.5	37.2	59.4
ttT	226189	865592	-TCE +TCE -TRK	26.9	9.7	8.5	41.4	18.8	27.6	23.6
ttT	236389	2531760	-TCE -TCE +TRK	22.8	9.3	55.9	70.3	46.2	57.8	17.7
ttT	228664	10556984	+CMUP-CMX -TRK	33.7	6.2	9.2	32.9	28.3	20.4	21.4
ttT	211396	9177382	-CMUP+CMX -TRK	44.7	21.1	7.8	29.2	25.8	38.9	41.1
tlT	194218	275349	+CMUP-CMIO+TRK	22.8	12.2	6.5	39.2	17.8	28.5	33.6
tlT	232812	7268361	+CMUP-CMIO-TRK	58.6	69.9	44.1	124.0	57.5	36.8	—

Table 17: We show some characteristics of the events we observe. In case of muons and tracks, E_T is the P_T of the object.

for the associated production of the chargino($\tilde{\chi}_1^{\pm}$) and neutralino($\tilde{\chi}_2^0$) with the signature being the distinctive three leptons + missing E_T signature. The MSSM model of supersymmetry is

characterized by over a 100 free parameters. Understanding this phase space is extremely difficult. The task can be significantly simplified by working within the constrained MSSM or mSUGRA. mSUGRA (as described in Section 1 is characterized by four parameters and one sign :

$$m_0,\ m_{1/2},\ A_0,\ \tan(\beta),\ \mathrm{sign}(\mu)$$

In this study we focus on the three paramters which give the most dramatic changes in the event kinematics and event topology - m_0,$m_{1/2}$ and $\tan(\beta)$.

The aim of this section is not to provide a comprehensive survey of all values of mSUGRA parameters, but rather to examine the dependence of analysis sensitivity to the different parameters.

We fix two of these parameters, $A_0 = 0$, and $\mu > 0$ for the present study. Variation of $\tan(\beta)$ leads to a variation of tau-lepton(τ) content in the decays of the chargino and neutralino. At higher values of $\tan(\beta)$, the decays of chargino and neutralino are dominated by τ's. Since this trilepton analysis does not include hadronic decays of τ's, we set $\tan(\beta)$ to a low value ($\tan(\beta)$=3) to reduce fraction of τ's in the final state. However, as we shall describe later, the dependence of final cross-section limits can be characterized by examining the τ content of the final state. We would be able to extract certain information about dependence of limits on $\tan(\beta)$ by studying the break-down of limits by τ content of the final state. Further updates of this note will include details.

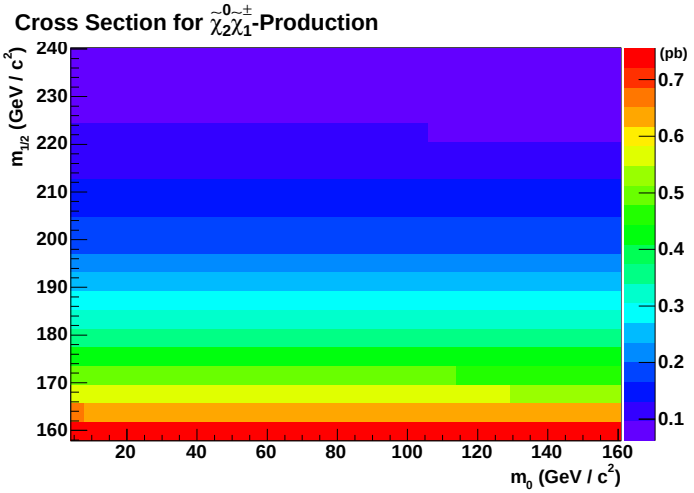

Figure 14: The figure shows the cross section of chargino neutralino production, $\sigma(p\bar{p} \rightarrow \widetilde{\chi}_1^\pm \widetilde{\chi}_2^0)$ in the $m_0 - m_{1/2}$ plane. The other mSUGRA parameters are kept constant at $\tan(\beta)$=3, A_0=0, μ >0. The σ is a smooth function of $m_{1/2}$. The bin size is 4 GeV/c^2 $\times$ 4GeV/c^2

We obtain the NLO cross-section for the signal process ($\sigma[p\bar{p} \rightarrow \widetilde{\chi}_1^\pm \widetilde{\chi}_2^0]$) from PROSPINO2[33] with input parameters fed from ISAJET 7.75. The branching ratio of $\widetilde{\chi}_1^\pm \widetilde{\chi}_2^0$ to trileptons (BR[$\widetilde{\chi}_1^\pm \widetilde{\chi}_2^0 \rightarrow l^\pm l^\mp l'^\pm$ + X]) is obtained from PYTHIA 6.409 based on the input parameters from ISAJET 7.75. The fully simulated Monte Carlo samples for signal are obtained by using Pythia 6.216 fed by ISAJET 7.51. This means that although we obtain the signal kinematic and acceptance from

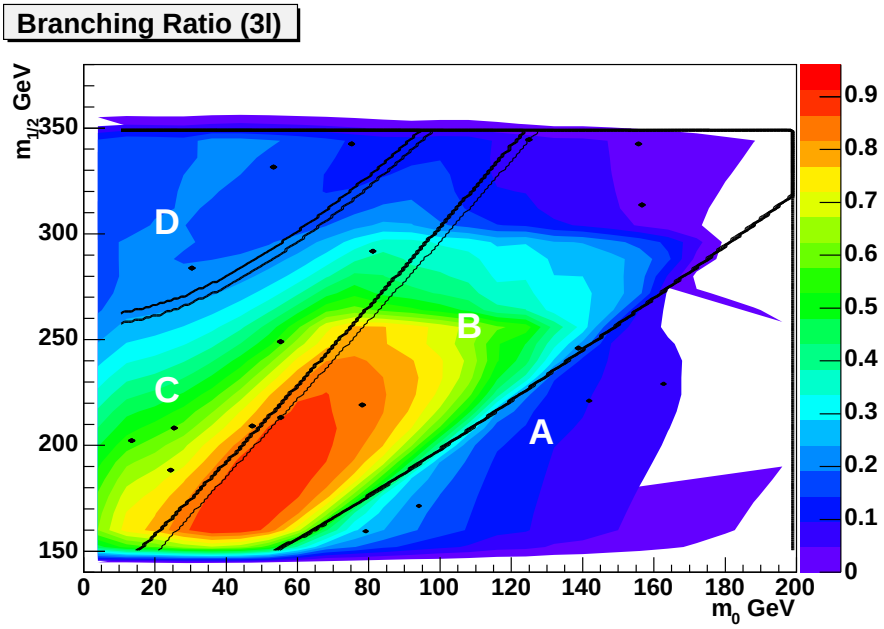

Figure 15: The figure shows the branching ratio to trileptons, BR($\widetilde{\chi}_1^{\pm}\widetilde{\chi}_2^0 \rightarrow$3l) in the $m_0 - m_{1/2}$ plane. The other mSUGRA parameters are kept constant at tan(β)=3, A_0=0, μ >0. The bin size is 10 GeV/c^2 $\times$ 10 GeV/c^2, although in certain places a finer grid is obtained.

ISAJET 7.51 and PYTHIA 6.216, and the theory parameters ($\sigma\times$BR) are obtained from later (and better) versions of ISAJET.

The σ is a smooth function of the mass of the $\widetilde{\chi}_1^{\pm}$(or $\widetilde{\chi}_2^0$), and thus depends very smoothly on $m_{1/2}$. This is shown in Figure 14. Far more interesting is the branching ratio of the $\widetilde{\chi}_1^{\pm}\widetilde{\chi}_2^0$ in to three leptons(BR[3l]). Figure 15 shows the BR[3l] in the $m_0 - m_{1/2}$ plane with other mSUGRA parameters fixed as described above. Before describing the features of this plot, it is worthwhile to refresh the decays of the $\widetilde{\chi}_1^{\pm}$and $\widetilde{\chi}_2^0$. The decays proceed via three-body or two-body decays. The three-body decays are straightforward, and gives the final trilepton state in the following way :
$\widetilde{\chi}_1^{\pm} \rightarrow l^{\pm}\nu\widetilde{\chi}_1^0$, and
$\widetilde{\chi}_2^0 \rightarrow l^{\pm}l^{\mp}\widetilde{\chi}_1^0$ where an intermediate virtual $W^{\pm}$ or Z boson or a virtual slepton is implied.
The two-body decays can proceed via intermediate slepton states as follows :
$\widetilde{\chi}_1^{\pm} \rightarrow \tilde{l}^{\pm}\ \nu$
$\widetilde{\chi}_2^0 \rightarrow \tilde{l}^{\pm}l^{\mp}$
where in each case the slepton decays to a lepton and the LSP, $\tilde{l} \rightarrow l\widetilde{\chi}_1^0$ or via real $W^{\pm}$ or Z decays as follows :
$\widetilde{\chi}_1^{\pm} \rightarrow W^{\pm}\widetilde{\chi}_1^0$, $W^{\pm} \rightarrow l^{\pm}\nu$
$\widetilde{\chi}_2^0 \rightarrow Z\widetilde{\chi}_2^0$, $Z \rightarrow l^{\pm}l^{\mp}$. The two-body decay branching ratios are thus sensitive to the mass of the sleptons. Let us now examine the various regions of Figure 15.

- Region **A** : This is the region where mass of the sleptons is higher than mass of the $\widetilde{\chi}_1^{\pm}$. The

decays of the $\widetilde{\chi}_1^{\pm}$ and the $\widetilde{\chi}_2^0$ proceed through a virtual or real $W^{\pm}$ or Z boson or virtual sleptons, and the branching ratio to the different flavors of leptons (e,μ,τ) are roughly equal.

- Region **B** : This is the region where mass of the right-handed sleptons ($\tilde{e}_R$, $\tilde{\mu}_R$, and $\tilde{\tau}_1$) is now below mass of the $\widetilde{\chi}_1^{\pm}$and $\widetilde{\chi}_2^0$. The two-body decays through sleptons enhance the overall branching ratio to leptons. The decays of the $\widetilde{\chi}_2^0$ to the three flavors of sleptons are roughly similar, but the $\widetilde{\chi}_1^{\pm}$ decays preferentially to $\tilde{\tau}$'s.

- Region **C** : In this region, the mass of the sneutrinos has also dropped below that of $\widetilde{\chi}_1^{\pm}$. The $\widetilde{\chi}_2^0$ can now also decay as follow $\widetilde{\chi}_2^0 \rightarrow \tilde{\nu}\nu$ which does not contribute to the trilepton signal.

- Region **D** : In this region, the mass of left-handed sleptons ($\tilde{e}_L$, $\tilde{\mu}_L$, and $\tilde{\tau}_2$) is less than mass of $\widetilde{\chi}_1^{\pm}$.

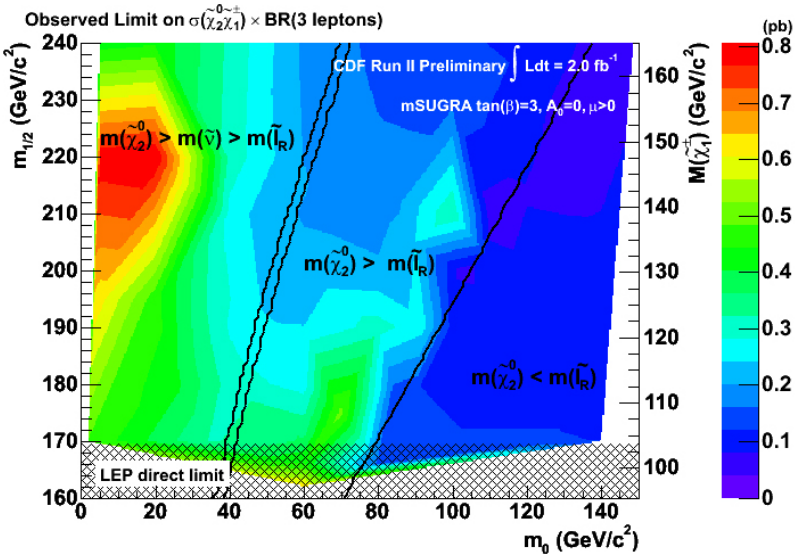

Figure 16: The figure shows the $\sigma\times$BR limits obtained from our result in the plane defined by m_0 and $m_{1/2}$. The regions are described in the text.

As seen from the figure, our sensitivity is maximum in Region B. This is the region we exploit to set limits shown in Figure 12 where m_0 is fixed at 60 GeV/c^2. Region A is intuitively easier to understand since decays are through $W^{\pm}$and Z (virtual or real) or virtual sleptons and are democratic to the three lepton flavors. We show these results in Figure 13 for $m_0 = 100$ GeV/c^2.

Figure 16 show the experimentally measured limits. By comparing the experimental limits to the theory expected cross-section $\times$ branching ratio, we can define an exclusion region in the $m_0 - m_{1/2}$ plane. We show the exclusion region in Figure 18. To obtain the exclusion contour we first obtain a list of excluded and non-excluded signal points. We then plot the the difference between theory $\sigma\times$BR and observed limits (Figure 17), and allow ROOT to interpolate between

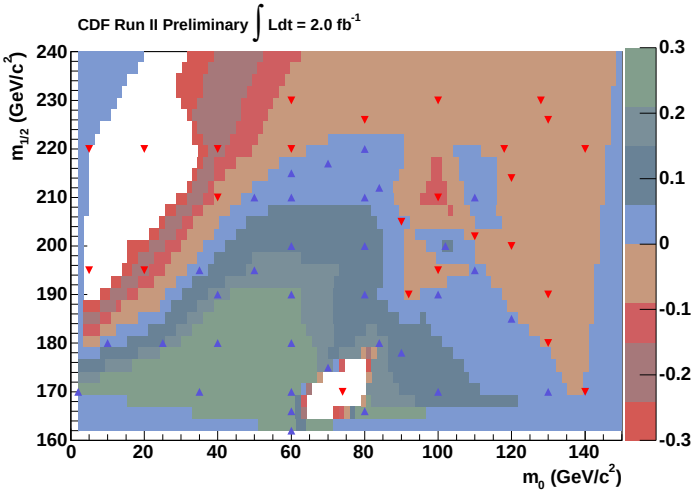

Figure 17: The figure shows the distribution of theory($\sigma\times$BR)$-$Observed limits on $\sigma\times$BR (in pb). The positive values represent excluded regions, and the negative values show non-excluded regions. Alternatively, the blue vertical triangles show excluded points, and the red upside-down triangles show the non-excluded points.

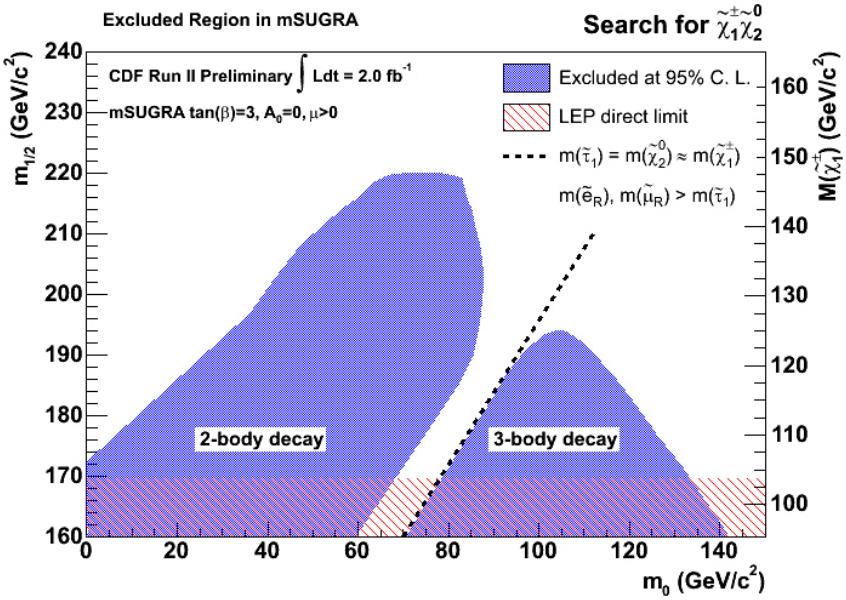

Figure 18: Figure shows exclusion region from this analysis in the $m_0 - m_{1/2}$ plane, with other mSUGRA parameters fixed as described. The LEP direct limit on chargino mass is also shown, along with lines representing significant mass relations. See text for more details.

negative (non-excluded) and positive (excluded) values of this difference to locate the zeros. The exclusion contour is then the locus of the zero difference between theory and observed 95% limits, i.e. the edge of exclusion region.

Figure 18 has two 'lobes' of exclusion. The right lobe (in region A from Figure 15) is in the region dominated by 3-body decays of $\widetilde{\chi}_1^{\pm}\widetilde{\chi}_2^0$. The left lobe (in region B,C from Figure 15) is in the region dominated by 2-body decays. The line representing small mass difference between $\widetilde{\chi}_1^{\pm}$(or $\widetilde{\chi}_2^0$) and sleptons is also shown. As we move closer to this line from Region B towards Region A, the sleptons get closer to the $\widetilde{\chi}_2^0$ in mass. The 2-body decay of the $\widetilde{\chi}_2^0$ ($\widetilde{\chi}_2^0 \rightarrow \tilde{l}^{\pm} l^{\mp}$) leads to a soft lepton. This causes the acceptance of the analysis to worsen and thus this region cannot be presently excluded. At the left edge of the left lobe, the mass of sneutrinos is getting smaller. This opens up the invisible decay of the neutralino ($\widetilde{\chi}_2^0 \rightarrow \tilde{\nu}\nu \rightarrow \nu\nu\widetilde{\chi}_1^0$). Hence the analysis acceptance drops and we cannot exclude this region.

For the sake of completeness we mention two other points. As we move to higher values of $m_{1/2}$ than discussed here, the production cross section of chargino-neutralino drops and consequently the sensitivity as well. As we move to higher m_0 values, the trilepton branching ratio drops to very small values and we lose sensitivity. This is shown in Figure 19.

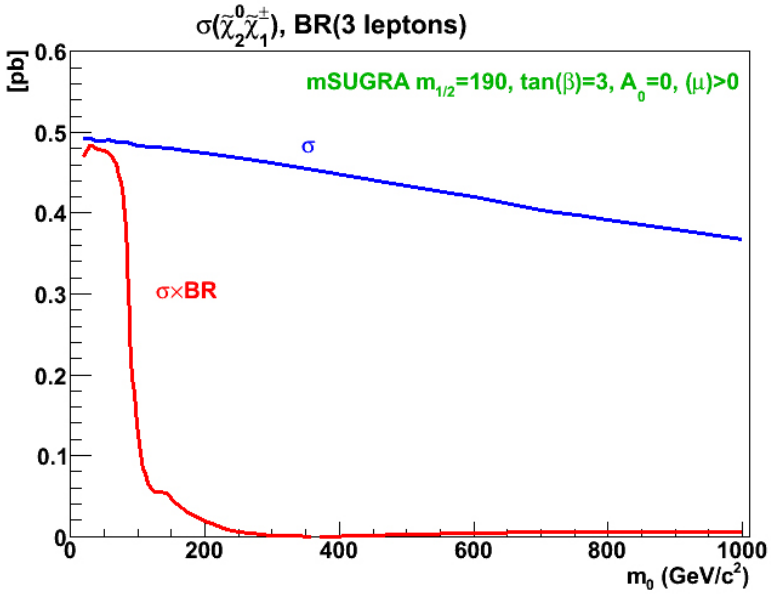

Figure 19: Figure shows cross section of chargino-neutralino production and the branching ratio to trileptons as a function of m_0 when the other mSUGRA parameters are fixed as indicated. At high m_0, the branching ratio is very small, and this analysis is not sensitive.

15 Acknowledgements

We thank John Zhou, Anadi Canepa, Else Lytken, Oscar Gonzales, Beate Heinemann, Giulia Manca, Vadim Rusu, Peter Wittich, Michael Gold, Vladimir Rekovic, John Strologas, Marcelo Vogel, Melisa Rossi, Giovanni Pauletta for their contributions.

We also want to thank current and former SUSY group and Exotic convenors for their leadership: Ben Brau, Chris Hays, Monica D'Onofrio, Dave Toback, Teruki Kamon, Stefan Lammel, Giulia Manca, Jane Nachtman, and Song Ming Wang.

Immense thanks to Ray Culbertson for his stntuple help and to Tom Junk for help with statistics.

We also thank our Rutgers colleagues Anton Anastassov, Eva Halkiadakis, Daryl Hare and Amit Lath.

References

[1] Searches for Chargino-Neutralino Production in mSUGRA Model in a Dielectron + Track Channel, J. Zhou, S. Dube, A. Lath, S. Somalwar. CDF7478

[2] Searches for Chargino-Neutralino Production in mSUGRA Model in a Dielectron + Track Channel, S. Dube, J. Zhou, A. Lath, S. Somalwar. CDF8098

[3] C. Quigg, "Gauge Theories of the Strong, Weak, and Electromagnetic Interactions," Addison-Wesley, Reading, MA, 1983, p. 188-189.

[4] R. Cahn, Rev. Mod. Phys. **68**, 951 (1996).

[5] J. L. Hewett, hep-ph/9810316 (unpublished).

[6] For a review, see e.g., H. Haber and G. Kane, Phys. Rept. **117**, 75 (1985).

[7] V. Barger, C. E. M. Wagner, *et al.*, "Report of the SUGRA Working Group for Run II of the Tevatron", hep-ph/0003154.

[8] G. R. Farrar and P. Fayet, Phys. Lett. B **76**, 575 (1978).

[9] H. Baer, C. Chen, F. Paige, and X. Tata, Phys. Rev. D **54** (1996) 5866; *op. cit.* **53** (1996) 6241; *op.cit.* **D52** (1995) 1565; **52** (1995) 2746; M. Machacek and M. Vaughn, Nucl. Phys. B **222** (1983) 83; C. Ford, D. Jones, P. Stephenson, and M. Einhorn, Nucl. Phys. B **395** (1993) 17.

[10] J. Ellis, S. Kelley, and D. Nanopoulos, Phys. Lett. B **260** (1991)131; P. Langacker and M. Luo, Phys. Rev. D **44** (1991) 817; U. Amaldi, W. deBoer, and H. Furstenau, Phys. Lett. B **260**(1991) 447; M. Carena, S. Pokorski, and C. Wagner, Nucl. Phys. B **406** (1993) 59; P. Langacker and N. Polonsky, Phys. Rev. D **47** (1993) 4028.

[11] Anna Lipniacka, "Can SUSY be found at Tevatron Run2?", hep-ph/0112280.

[12] http://lepsusy.web.cern.ch/lepsusy/

[13] A. Faessler, R. Kosmas, S. Kovalenko, and J. Vergados, Nucl.Phys. **B587**, 25 (2000).

[14] Search for Chargino-Neutralino Production in $p\overline{p}$ Collisions at $\sqrt{s} = 1.96$ TeV, T. Aaltonen *et al.*, PhysRevLett.99.191806

[15] Search for Supersymmetry via Associated Production of Charginos and Neutralinos in Final States with Three Leptons, V. Abazov *et al.*, PhysRevLett 95 151805

[16] http://www-cdf.fnal.gov/internal/dqm/goodrun/good.html

[17] J. M. Campbell and R. K. Ellis; next-to-leading-order calculation using MCFM version 3.4.5. Phys. Rev. D **60** (1999) 113006.

[18] M. Cacciari, S. Frixione, G. Fidolfi, M. Mangano and P. Nason, JHEP **404**(2004) 68.

[19] http://www-cdf.fnal.gov/physics/new/top/top.html shows the results for $t\bar{t}$ cross section measurement from CDF. We use a combined number from different analyses with 350 pb^{-1} of data.

[20] "Measurement of the Inclusive $b\bar{b}$ jet production cross section", A. Gajjar, R. McNulty, A. Mehta, T. Shears.

[21] Generic Jet Corrections for Run II, F. Canelli, A. Bhatti. CDF7358

[22] Low E_T electron ID efficiency and scale-factors using J/Ψ, S. Dube, J. Zhou, S. Somalwar. CDF7379

[23] Medium E_T electron identification efficiency and scale-factors, S. Dube, J. Zhou, S. Somalwar. CDF8321

[24] The fractional track isolation is a ratio of : The scalar sum of tracks with $p_T > 0.4$ GeV within a cone of 0.4 in $\eta - \phi$ space around the track in consideration, and the p_T of the track in consideration. All surrounding tracks must also satisfy $|z_v^{\rm surroundingtrack} - z_v^{\rm candidatetrack}| < 4$ cm. A requirement of 0. fractional isolation means requiring that there are no $\geq$0.4 GeV tracks in a cone of 0.4 around the primary track.

[25] Central Electron ID Efficiencies at Medium Energy, G. Manca, B. Heinemann, G. Martin. CDF7233

[26] Electron Identification in Offline Release 5.3, C. Hill, J. Incandela, and C. Mills. CDF7309

[27] Electron Identification in Offline Release 6.1.2, T. Spreitzer, C. Mills, J. Incandela. CDF7950

[28] Measuring Central Electron Trigger Efficiencies for 4 GeV Triggers, S. Dube, J. Zhou, S. Somalwar. CDF7095

[29] Low p_T Muon ID efficiencies and Scale Factors for Exotics Searches, M. Gold, V. Rekovic. CDF7210

[30] Low p_T Muon Isolation Efficiency and Scale Factors, M. Gold, V. Rekovic. CDF7432

[31] High-Pt Muon ID Cuts and Efficiencies for use with 5.3.1 Data and 5.3.3 MC, V. Martin. CDF7367

[32] First Measurements of Inclusive W and Z Cross Sections from Run II of the Tevatron Collider, D. Amidei, *et al.*. CDF7332

[33] The Production of Chargions/Neutralinos and Sleptons at Hadron Colliders, W. Beenakker, *et al.*, Phys. Rev. Lett. **83** (1999) 3780-3783.

[34] CTEQ6, J. Pumplin, D. R. Stump, J. Huston, H. L. Lai, P. Nadolsky and W. K. Tung, JHEP 0207, 012 (2002).

[35] Search for Gluinos and Squarks Using Like-Sign Dilepton Events, J. Done, M. Chertok, T. Kamon. CDF4909

[36] Acceptance and background systematics for the Top Dilepton cross-section measurement, M. Tecchio. CDF6590

[37] Measurement of ZZ+ZW cross section using Run II data, S. Cabrera, J. Deng, A. Goshaw, C. Hays, Y. Huang, M. Kruse. CDF6920

[38] Search for the associated production of chargino and neutralino in the final state with two muons and an additional lepton, D. Bortoletto, A. Canepa, O. Gonzalez, E. Lytken. CDF8114

[39] Searches for Chargino and Neutralino in the e+e/mu+e/mu with 1 fb-1 of data, G. Manca, M. Griffiths, B. Heinemann CDF8389

[40] Efficiency of the Z-vertex cut of 60 cm for 2002-2006 data , http://www-cdf.fnal.gov/internal/physics/joint_physics/instructions/zvertex-efficiency.html

[41] PerfIDia, http://ncdf70.fnal.gov:8001/PerfIDia/PerfIDia.html

[42] Searches for Chargino-Neutralino Production in mSUGRA model in a Di-electron + Track Channel, S. Dube, J. Zhou, A. Lath, S. Somalwar CDF8445

[43] Search for chargino-neutralino production in the inclusive low-pT dimuon+lepton channel with 1 fb-1, M. Gold, V. Rekovic, J. Strologas CDF8479

[44] http://www-cdf.fnal.gov/tiki/tiki-index.php?page=EwkDatasets

[45] Photon Conversion Removal Efficiency, A. Attal, A. Canepa CDF8073

[46] Level 1, 2, and 3 Low pT Muon Trigger Efficiencies in gen6 Data for the SUSY Trilepton Searches, M. Gold, V. Rekovic, J. Strologas CDF8308

[47] Fake Rate For Low-p_T Leptons, G. Manca, M. Griffiths, B. Heinemann CDF7470

[48] Search for ZZ in the 4 lepton and dilepton + MET channel and update of WZ in the trilepton +MET, S.-C. Hsu, E. Lipeles, M. Neubauer, M. Norman, R. Vanguri, F. Wurthwein, CDF8924

[49] Measurement of the top quark mass in the dilepton channel 2.0/fb with the Matrix-Element Method, B. Jayatilaka, A. Kotwal, R. Shekhar, D. Whiteson, M. Tecchio, CDF9098

[50] http://www-cdf.fnal.gov/ dube1/internal/susyana

A Appendix : Isolated Track Rate

A major background in the dilepton+track channels is from events where the two primary leptons come from SM processes and the track comes from the underlying event or from a jet where one charged particle showers outside the core of the jet. Hence we need to measure the rate for this process.

A.1 Measuring the isolated track rate

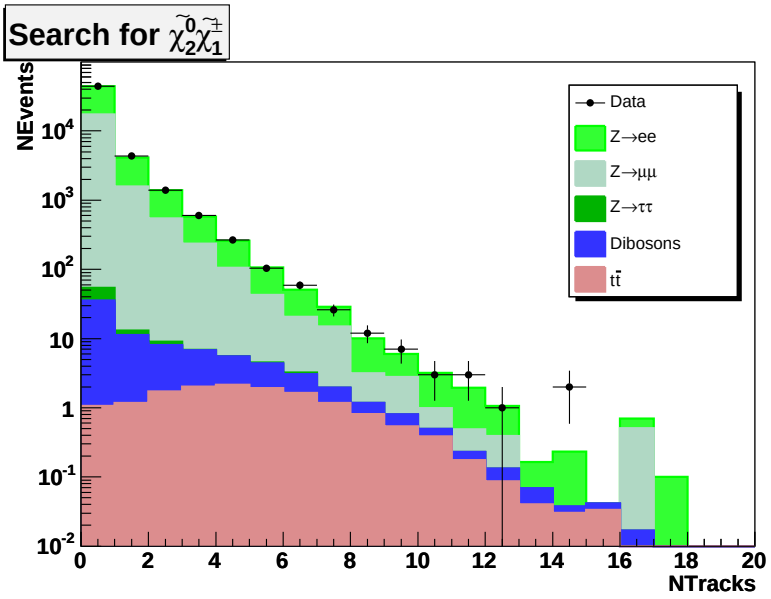

Figure 20: Track multiplicity for **tt** Z events. Z selection is discussed elsewhere in the text.

We measure the rate of an isolated track per event using Z data from the High P_T datasets bhel and bhmu.

The measurement procedure is:

- Select $Z \to ee$ and $Z \to \mu\mu$ events with two tight leptons[3]. Mass Window: $|M_{ll} - 91.2| < 15$ GeV.
- Require $\not\!\!E_T < 10$ GeV to remove WZ and $t\bar{t}$ contributions. All other SM contribution is negligible[4].
- Count the number of events with at least one extra isolated track as a function of number of good tracks (NAxSeg>2,NStSeg> 2,TrkP$_{\rm T}$ > 4 GeV,$|Z_0| < 60$cm, within 5cm of event vertex) excluding the two tracks which form the invariant mass.

[3]See Section 4 for tight lepton requirements.
[4]Reference [32] shows that the total background is < 1%.

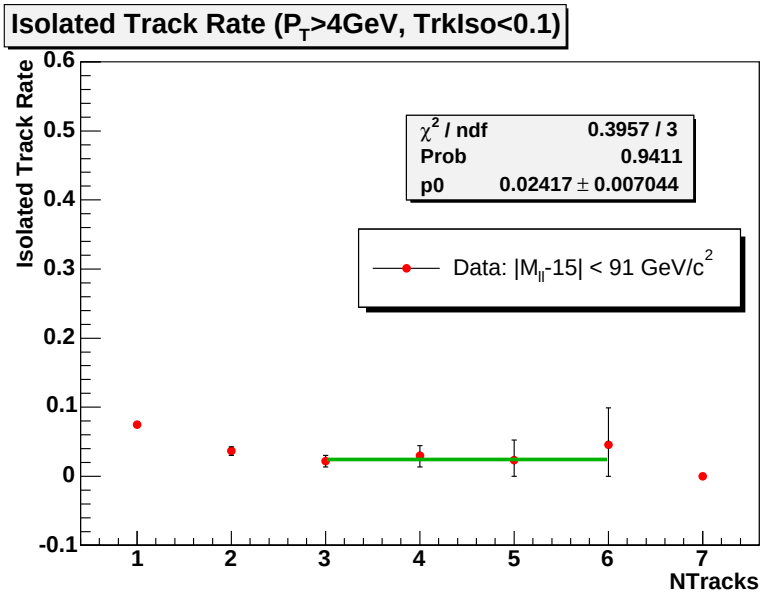

Figure 21: Isolated track rate in Z events in entire dataset. The fit is ITR(NTrk)=p_0 for NTrk>2. For NTrk=1, the track rate is $= 0.075 \pm 0.005$. For NTrk=2, the track rate is $= 0.037 \pm 0.006$.

Figure 20 shows the track multiplicity distributions for the Z events. Figure 21 shows the Isolated Track Rate (ITR) for the Z data. The track rate is fit with a straight line for events with more than two track.

A.2 Applying isolated track rate

To estimate the number of expected dilepton+track events in our sample, we apply the ITR measured with data Z events to MC as follows:

- The MC events must have two tight leptons as described before.
- If there is no third isolated track or it is not matched to a hepg lepton, the ITR is applied to the MC event as a weight.

The measured ITR from Z data is applicable to DY, WW, WZ, and ZZ events.
The event acceptance is then:

$$Acc = \frac{(N^{cut}_{3lep} * \epsilon^{cut}_{3lep} + N^{cut}_{3lep}/N^{base}_{3lep} * N_{dilep} * \epsilon_{dilep})}{N_{gen}}, \quad (1)$$

where ϵ is the average event weight, "*base*" stands for dilepton+track cut, and "*cut*" stands for additional cuts on top of the "*base*" cuts. Therefore $N^{cut}_{3lep}/N^{base}_{3lep}$ stands for the efficiency for a particular optimized cut for an event with 2 leptons and a track. The corresponding ϵ^{cut}_{3lep} is the

average event weight for events passing "*cut*". The average event weight includes lepton ID scale factors and trigger efficiency. "N_{gen}" is the number of generated MC events. "N_{dilep}" stands for dilepton only events. ϵ_{dilep} includes the ITR weight in addition to lepton ID scale factor and trigger efficiency. The error on *Acc* is then propagated with the errors of individual ϵ and the binomial errors of N_{3lep}^{cut}/N_{gen}, $N_{3lep}^{cut}/N_{3lep}^{base}$, and N_{dilep}/N_{gen}.

B Appendix : Lepton Fake Rates

In this section we show the fake rates for our tight and loose lepton categories. The measurement method is described in [47]. The measurement description will be released in a separate note. Figure 22 shows the fake rates for the various lepton categories.

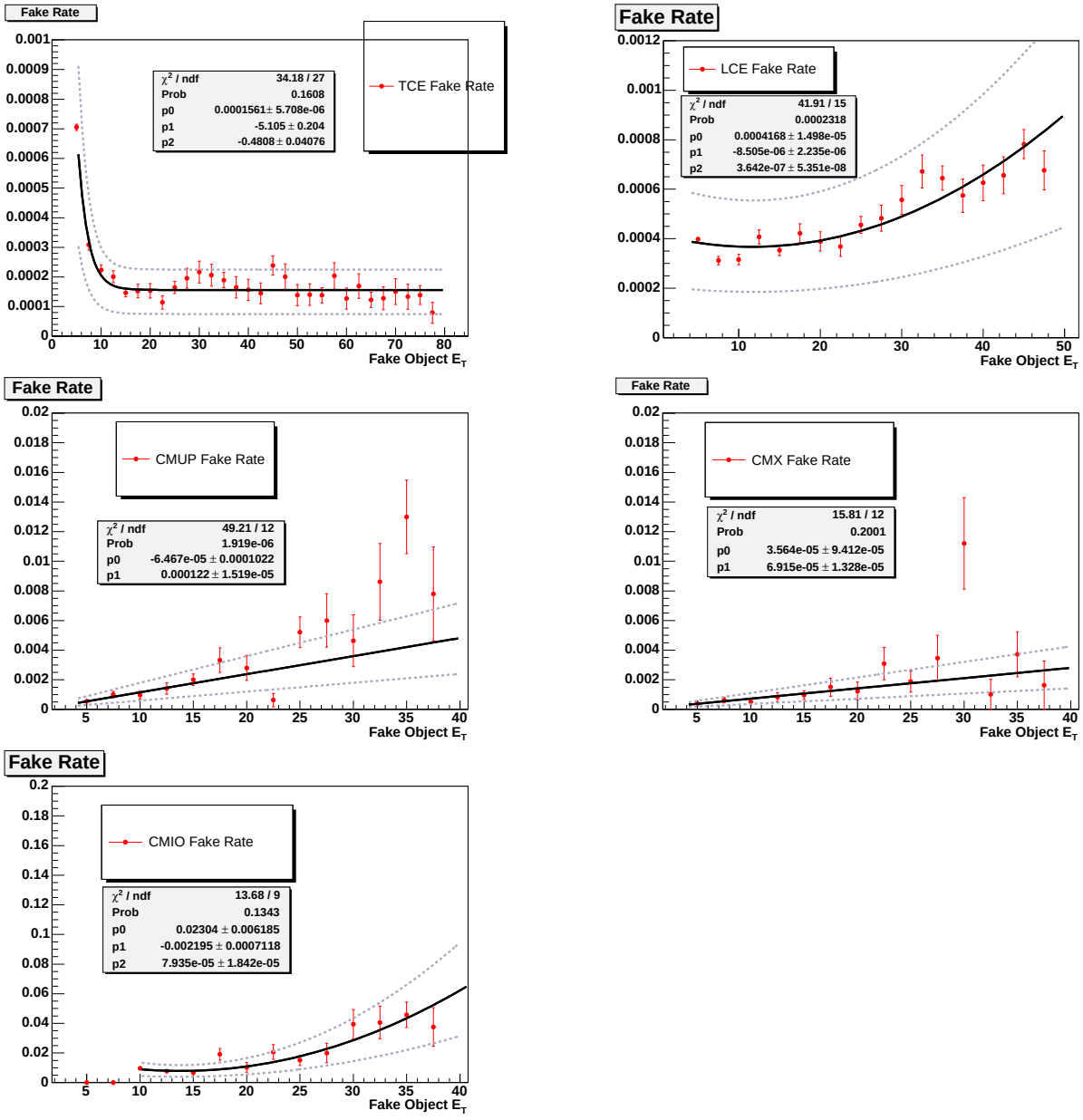

Figure 22: Figure shows the fake rates for top left: TCE, top right: LCE, middle left: CMUP, middle right:CMX bottom: CMIO .Fits to the points are shown along with the 50% systematic that we take.

C Appendix : All Control Region Numbers

In this section we show the control regions predictions and observed events for all of our control regions. Table 18 shows the numbers for the dilepton control regions. The numbers for certain

regions by lepton flavor are also shown. In the table, the control region eμ refers to following selection - One electron, One muon. For the eμ control region, we do not split into Z and Zveto, or high and low $\not\!\!E_T$.

Table 19 shows the control region numbers for the trilepton control regions, Table 20 shows the same for the dilepton+track control regions.

D Appendix : Systematics for all channels

In this section we show the full systematics for all of our channels. Tables 21 and 22 follow the tables of systematics described in previously. The numbers in brackets indicate the numbers for ttC and tll in case of trilepton table and for tlT$_\tau$ in case of dilepton+track table.

E Appendix : Kinematic variables in control region Z

In this section, we show a few kinematic distributions in the control region Z ($76 < \mathrm{M_{ll}} GeV/c^2 < 106$). Figure 23 shows the distributions for tt category, figure 24 for the tl category. Figure 25 shows the distributions for ttt category, figure 26 for the ttT_τ category.

Name	Z→ ee	Z→ $\mu\mu$	Z→ $\tau\tau$	WW	WZ	ZZ	$t\bar{t}$	Background	Observed
tt									
!Z	9847.8	5034.7	1310.2	93.3	1.6	7.1	57.1	16352 ± 716	15966
!Zlo	7705.6	4240.6	477.7	4.7	0.1	2.3	1.0	12432 ± 569	12352
!Zhi	858.4	205.5	550.3	83.5	1.4	3.6	55.0	1758 ± 80	1612
Z	31178.2	19870.4	21.9	22.4	6.3	35.8	15.0	51150 ± 2034	51042
Zlo	25577.6	16665.6	11.1	1.6	0.2	13.4	0.2	42270 ± 1682	42093
Zhi	1261.1	741.5	6.4	19.0	5.8	15.9	14.4	2064 ± 92	2143
lo	33349.6	20903.9	488.7	6.3	0.3	15.7	1.2	54766 ± 2212	54445
Z(ee)	31178.3	0.0	6.7	6.5	4.0	21.9	4.7	31222 ± 1710	31074
Z($\mu\mu$)	0.0	19867.7	3.9	4.6	2.3	13.9	3.0	19895 ± 1102	19942
!Z(ee)	9847.9	0.0	497.8	29.9	1.1	4.3	18.3	10399 ± 617	10033
!Z($\mu\mu$)	0.0	5015.4	243.2	18.2	0.4	2.3	10.9	5290 ± 352	5198
eμ	-0.2	21.9	580.4	56.5	0.1	0.5	35.1	694 ± 47	761
tl									
!Z	1979.7	4360.1	740.7	69.5	0.4	3.8	44.1	7198 ± 300	7069
!Zlo	1281.8	3516.7	318.8	3.5	0.0	1.3	0.8	5123 ± 234	5147
!Zhi	383.1	258.1	259.7	62.2	0.4	1.9	42.4	1008 ± 46	976
Z	11245.7	30953.7	24.0	19.6	4.7	27.1	13.1	42288 ± 1868	41833
Zlo	9061.3	25901.2	13.7	1.5	0.2	10.2	0.3	34988 ± 1557	35055
Zhi	538.4	1177.5	6.6	16.7	4.3	12.0	12.5	1768 ± 85	1616
lo	10342.5	29417.5	332.5	5.0	0.2	11.4	1.0	40110 ± 1776	40202
Z(ee)	10572.3	0.0	5.5	2.8	1.3	7.0	1.9	10591 ± 664	10235
Z($\mu\mu$)	0.0	30906.7	6.5	6.5	3.4	19.6	4.2	30947 ± 1728	30958
!Z(ee)	1706.5	0.0	132.0	9.2	0.1	1.1	6.0	1855 ± 114	1890
!Z($\mu\mu$)	0.0	4285.8	223.9	23.1	0.3	2.4	14.2	4550 ± 261	4482
eμ	946.1	121.3	396.9	47.5	0.1	0.8	30.8	1543 ± 72	1337

Table 18: Table shows the control region numbers for all dilepton regions.Same-sign events are subtracted in data to estimate the number of one lepton + one fake events. Errors include MC statistics, and partial systematics such as lepton ID, trigger efficiencies and Drell Yan cross-section uncertainty of 5%

Name	Z→ ee	Z→ $\mu\mu$	Z→ $\tau\tau$	WW	WZ	ZZ	$t\bar{t}$	Fakes	Background	Observed
ttt										
lo	7.58	2.92	0.00	0.00	0.05	0.57	0.00	6.01	17.13 ± 5.32	17
!Zlo	3.73	1.25	0.00	0.00	0.04	0.17	0.00	1.14	6.33 ± 2.71	9
Z	4.67	2.17	0.00	0.01	1.30	0.82	0.02	7.68	16.66 ± 5.71	9
Zlo	3.86	1.67	0.00	0.00	0.01	0.40	0.00	4.87	10.81 ± 4.21	8
Zhi	0.00	0.09	0.00	0.01	1.23	0.30	0.02	1.06	2.71 ± 1.73	0
ttC										
lo	0.74	3.38	0.00	0.00	0.04	0.31	0.00	2.57	7.03 ± 3.02	9
!Zlo	0.64	1.09	0.00	0.00	0.02	0.10	0.00	0.33	2.17 ± 1.54	3
Z	0.10	2.69	0.00	0.00	1.09	0.64	0.01	3.13	7.66 ± 3.23	8
Zlo	0.10	2.29	0.00	0.00	0.02	0.21	0.00	2.24	4.86 ± 2.52	6
Zhi	0.00	0.08	0.00	0.00	1.05	0.34	0.01	0.28	1.76 ± 1.34	2
tll										
lo	0.57	1.81	0.00	0.00	0.03	0.19	0.00	1.68	4.28 ± 2.28	3
!Zlo	0.12	0.96	0.00	0.00	0.00	0.07	0.00	0.29	1.44 ± 1.25	0
Z	0.64	1.09	0.00	0.00	0.70	0.32	0.02	2.63	5.41 ± 2.70	6
Zlo	0.45	0.84	0.00	0.00	0.03	0.12	0.00	1.39	2.83 ± 1.86	3
Zhi	0.19	0.09	0.00	0.00	0.62	0.14	0.02	0.57	1.62 ± 1.31	2

Table 19: Table shows the control region numbers for all trilepton regions. Systematic errors are being evaluated

F Appendix : Kinematic variables in control region !Z

In this section, we show a few kinematic distributions in the control region !Z ($M_{ll} < 76 GeV/c^2$ or $M_{ll} > 106 GeV/c^2$). Figure 27 shows the distributions for tt category, figure 28 for the tl category.

Name	Z→ ee	Z→ $\mu\mu$	Z→ $\tau\tau$	WW	WZ	ZZ	$t\bar{t}$	Fakes	Background	Observed
ttT_τ										
lo	168.37	138.84	1.73	0.02	0.02	0.35	0.02	2.39	311.75 ± 34.53	290
!Zlo	49.31	35.84	1.61	0.01	0.01	0.10	0.00	1.57	88.45 ± 12.95	72
Z	166.42	140.97	0.12	0.13	0.32	0.77	0.29	1.82	310.84 ± 34.45	299
Zlo	119.06	103.00	0.12	0.01	0.01	0.25	0.02	0.83	223.30 ± 26.20	218
Zhi	14.67	10.40	0.00	0.09	0.30	0.41	0.27	0.67	26.82 ± 6.03	34
tlT_τ										
lo	55.02	170.96	0.74	0.01	0.01	0.24	0.05	1.37	228.40 ± 29.97	214
!Zlo	6.64	25.38	0.74	0.00	0.00	0.08	0.03	0.90	33.78 ± 7.17	31
Z	69.45	202.01	0.15	0.11	0.27	0.56	0.30	1.13	273.97 ± 35.15	246
Zlo	48.38	145.58	0.00	0.01	0.00	0.15	0.02	0.47	194.62 ± 26.31	183
Zhi	8.59	17.69	0.00	0.10	0.27	0.32	0.28	0.48	27.74 ± 6.38	23

Table 20: Table shows the control region numbers for all dilepton+track regions. Fake event contributions for the dilepton+track channels are included in the other predictions (see section A). Systematic errors are being evaluated

G Appendix : Kinematic variables in control region lo$\not\!\!E_T$

In this section, we show a few kinematic distributions in the control region lo $\not\!\!E_T$ ($\not\!\!E_T \leq 10GeV$). Figure 29 shows the distributions for tt category, figure 30 for the tl category.

Sample	ID	Trig	JES	Conv	Xsec	PDF	ISR/FSR
Z→ee	4	0.5	2(8)	16	5	4.1	4
Z→ $\mu\mu$	4	0.5	6(8)	5(10)	5	4.1	4
Z→ $\tau\tau$	4	0.5	4(11)	0	5	4.1	4
WW	4	0.5	0.5	0	10	2	4
WZ/γ^*	4	0.5	2.9	4	10	2.7	4
ZZ	4	0.5	0.8(1.4)	1	10	2.7	4
$t\bar{t}$	4	0.5	12(15)	3	15	2	4
Fake	0	0	0	0	50	0	0
Signal	4	0.5	0.5	-	10	2	4

Table 21: Systematic errors (in percentage) for ttt channels. A universal 6% uncertainty on the luminosity is not included in this table.

Sample	ID	Trig	JES	ITR(nom)	ITR(alt)	Xsec	PDF	ISR/FSR
Z→ee 4	0.5	12.8	20	4(23)	5	4.1	4	
Z→ $\mu\mu$	4	0.5	22	20	4(23)	5	4.1	4
Z→ $\tau\tau$	4	0.5	8.3	10	10(27)	5	4.1	4
WW	4	0.5	0.5	10	11(24)	10	2	4
WZ/γ^*	4	0.5	0.5	5	60	10	2.7	4
ZZ	4	0.5	0.8	5	60	10	2.7	4
$t\bar{t}$	4	0.5	12	10	60	15	2	4
Fake	4	0.5	0	0	0	50	0	4
Signal	4	0.5	1.2	-	-	10	2	4

Table 22: Systematic errors (in percentage) for ttT_τ channel. A universal 6% uncertainty on the luminosity is not included in this table.

H Appendix : Kinematic variables in control region !Zhi

In this section, we show a few kinematic distributions in the control region !Zhi ($M_{ll} < 76GeV/c^2$ or $M_{ll} > 106GeV/c^2$ and $\not\!\!E_T \geq 15$ GeV). Figure 31 shows the distributions for tt category, figure 32 for the tl category.

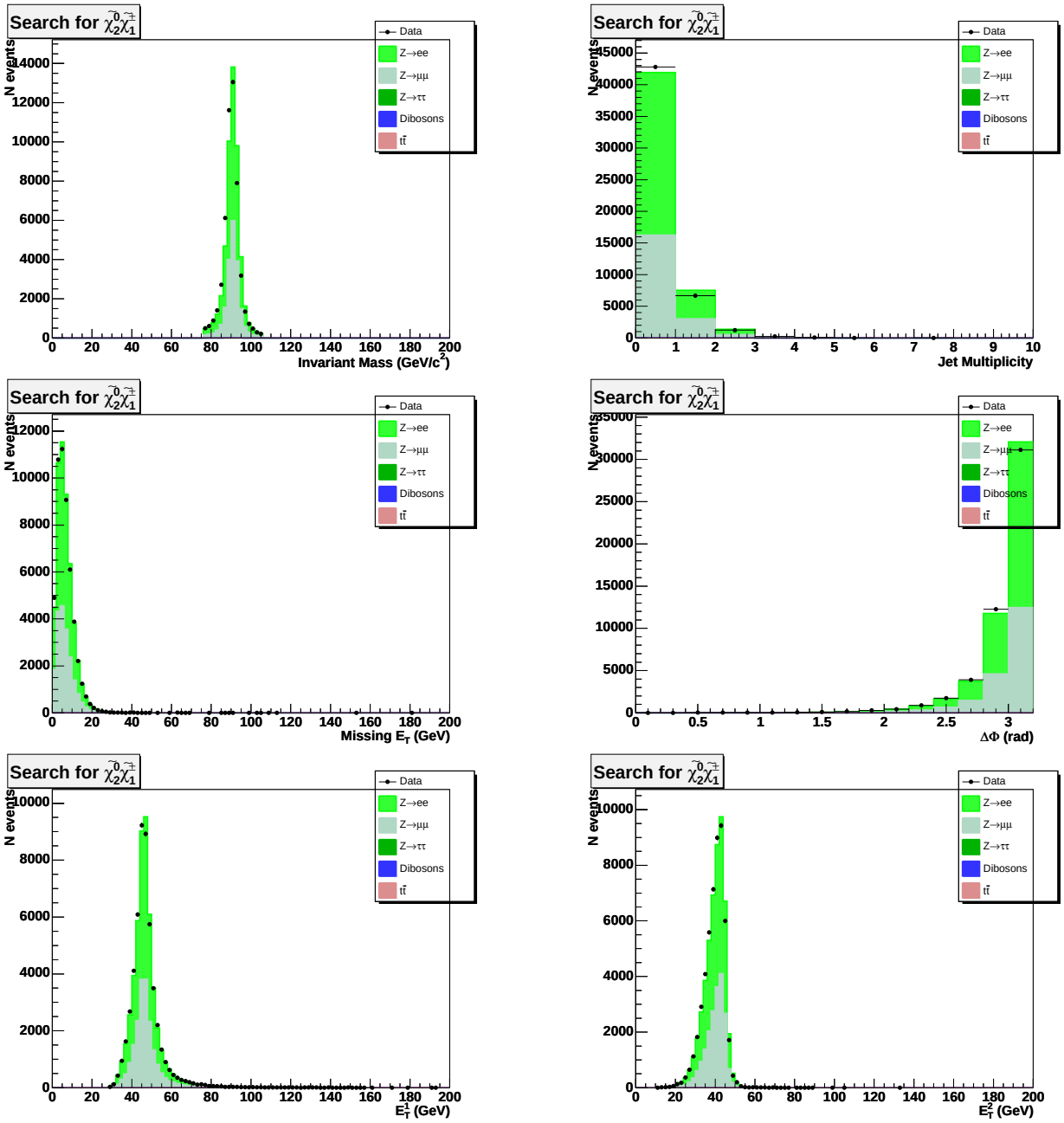

Figure 23: M_{ll}, njets, missing energy, $\triangle\phi_{lep12}$, leading and trailing lepton E_T. distributions in control region Z with 2 tight leptons. Points are data and stacked histograms are background expectation.

I Appendix : Kinematic variables in control region Zhi

In this section, we show a few kinematic distributions in the control region Zhi ($76 < M_{ll} GeV/c^2 < 106$ and $\not\!\!E_T \geq 15$ GeV). Figure 33 shows the distributions for ttC category, figure 34 for the ttT_τ

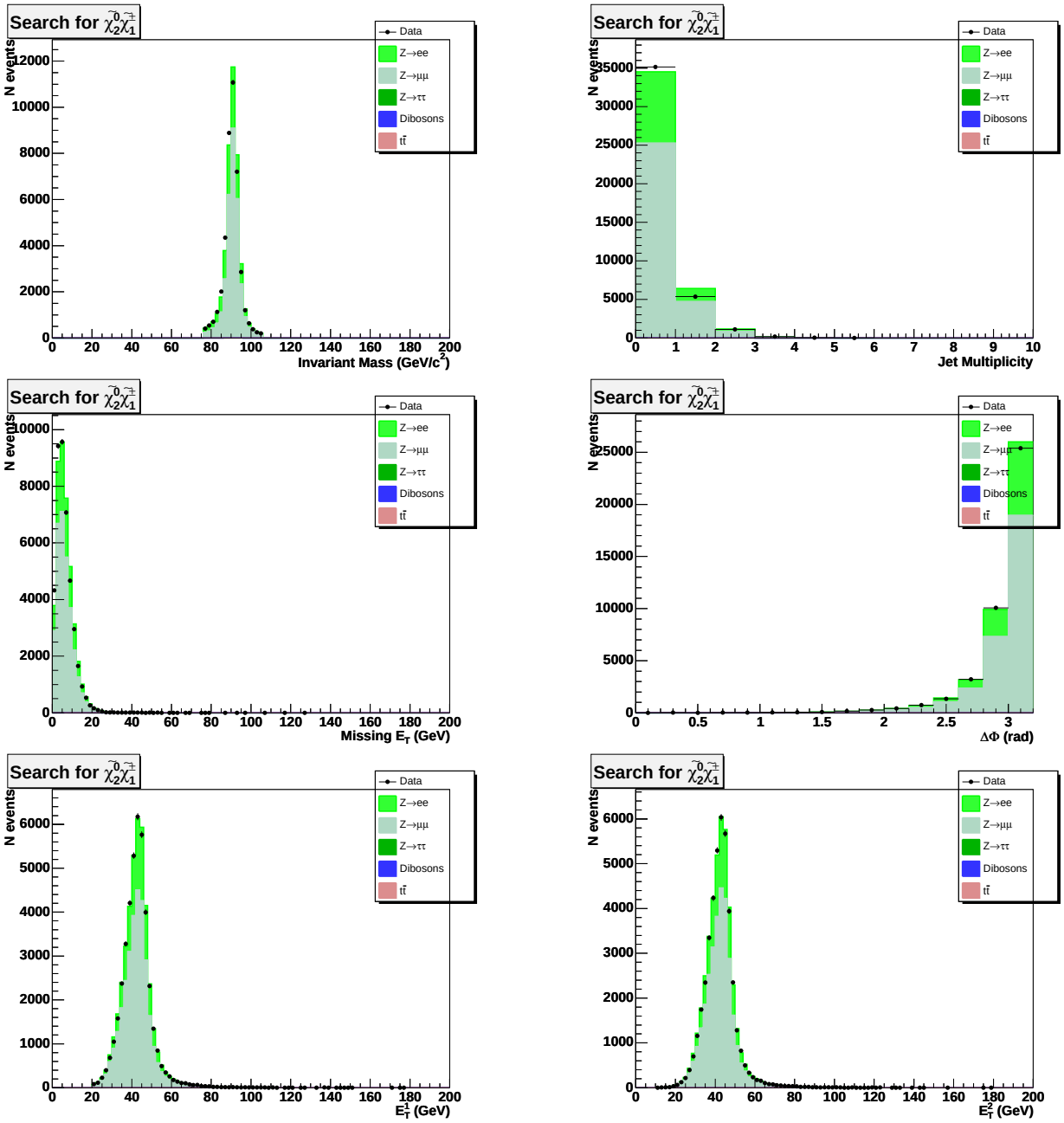

Figure 24: M_{ll}, njets, missing energy, $\triangle\phi_{lep12}$, leading and trailing lepton E_T. distributions in control region Z with 1 tight + 1 loose leptons. Points are data and stacked histograms are background expectation.

category.

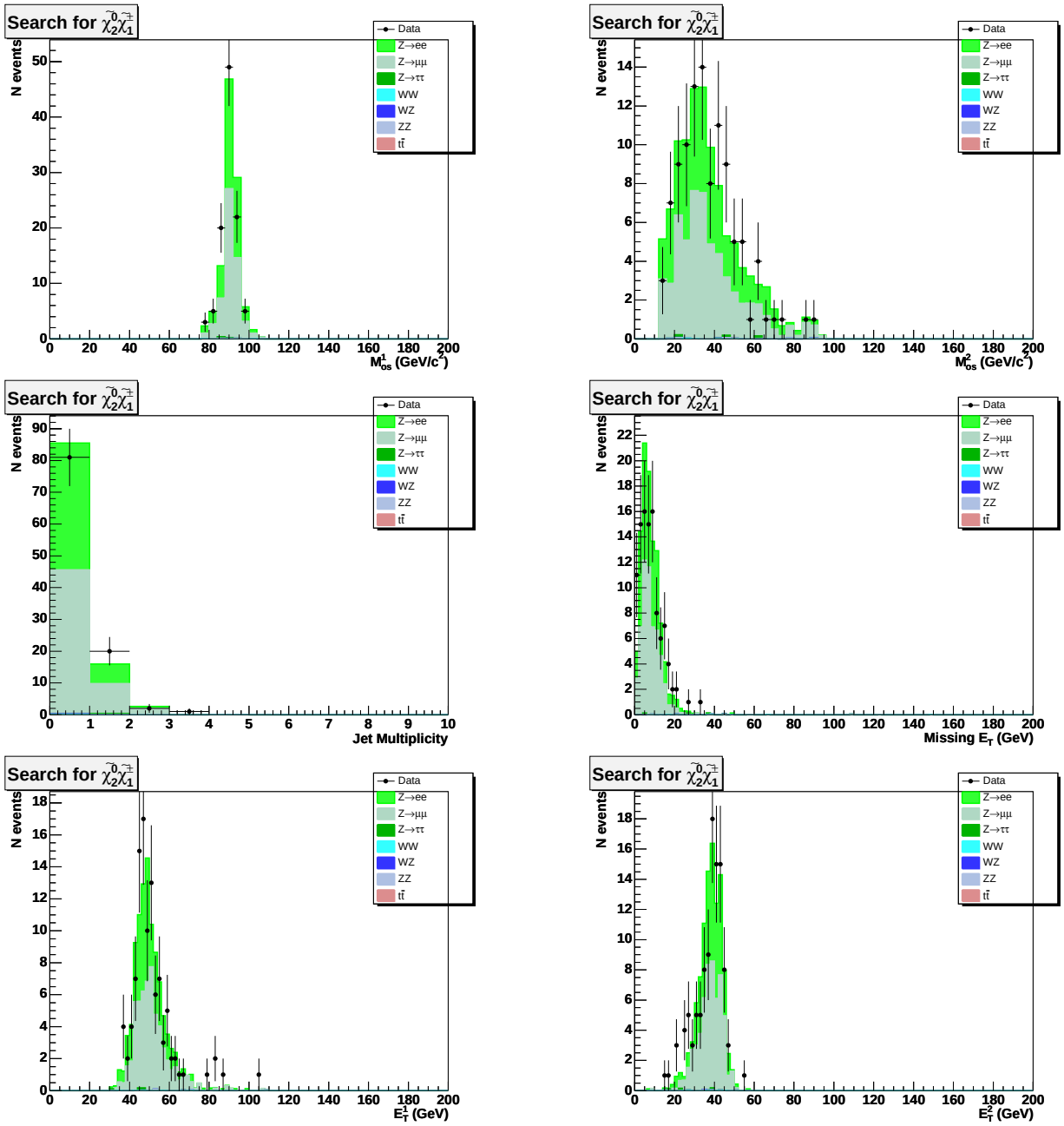

Figure 25: M_{ll}, njets, missing energy, leading lepton E_T distributions in control region Z with 3 tight leptons. Points are data and stacked histograms are background expectation.

J Appendix : Kinematic variables in control region Z by lepton flavor

In this section, we show a few kinematic distributions in the control region Z (dileptons) ($76 < M_{ll} GeV/c^2 < 106$) with a split into electron and muon pairs. Figure 35 shows the distributions for

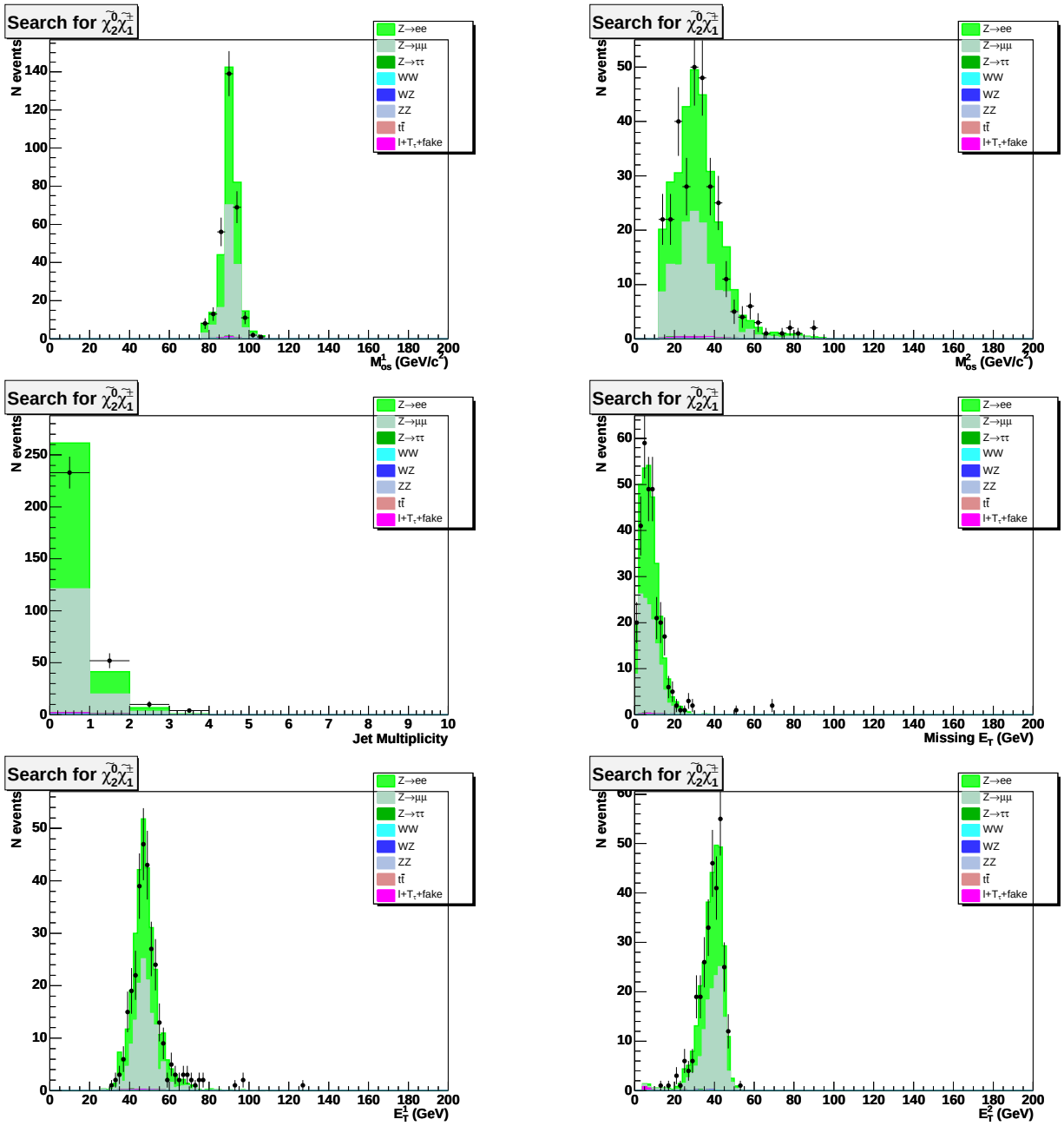

Figure 26: M_{ll}, njets, missing energy, leading lepton E_T distributions in control region Z with 2 tight lepton + 1 isolated track. Points are data and stacked histograms are background expectation.

electron pairs, figure 36 for muon pairs.

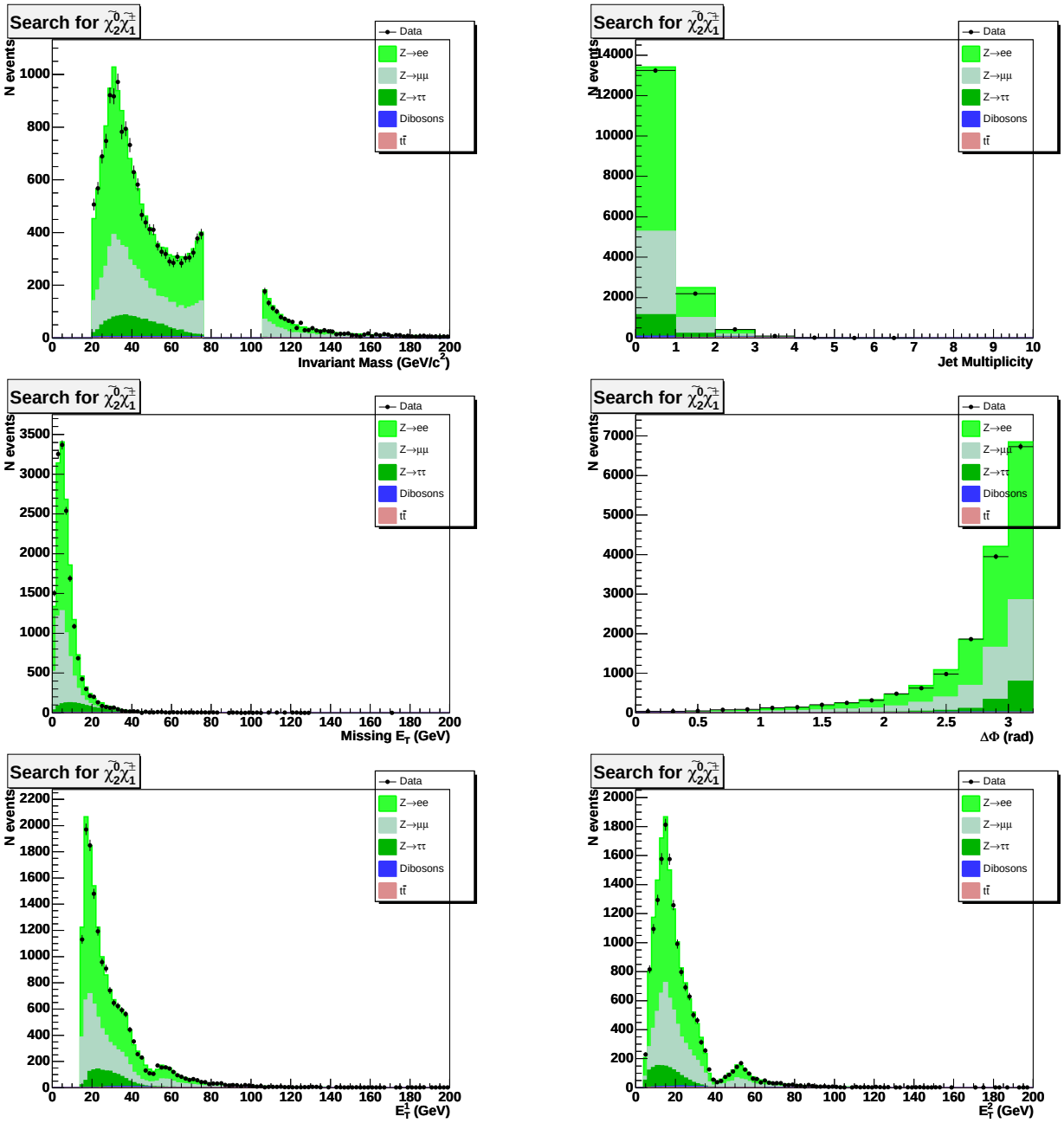

Figure 27: M_{ll}, njets, missing energy, $\triangle\phi_{lep12}$, leading and trailing lepton E_T. distributions in control region !Z with 2 tight leptons. Points are data and stacked histograms are background expectation.

K Appendix : Kinematic variables in control region !Z by lepton flavor

In this section, we show a few kinematic distributions in the control region !Z (dileptons) ($M_{ll} < 76GeV/c^2$ or $M_{ll} > 106GeV/c^2$) with a split into electron and muon pairs. Figure 37 shows

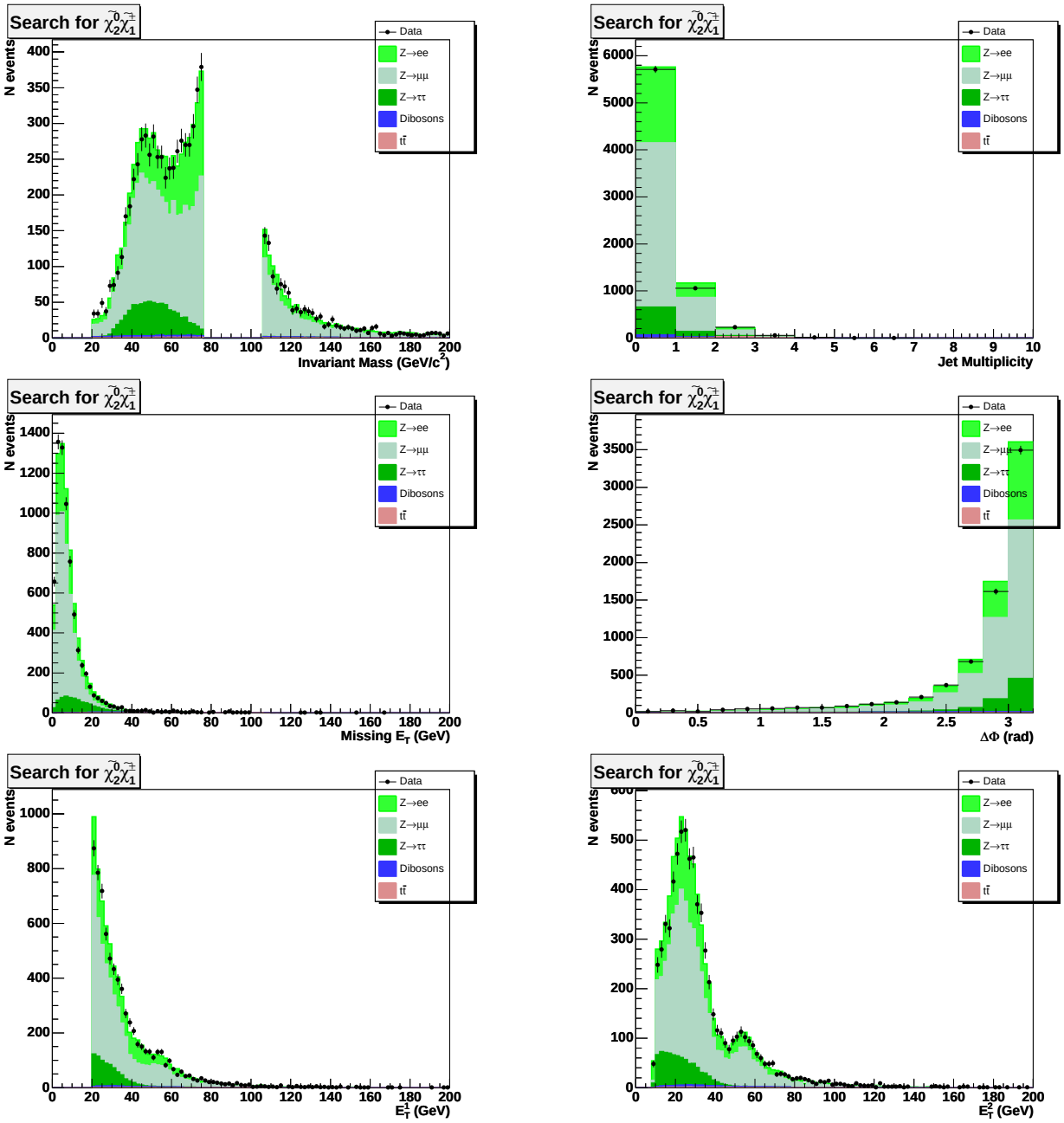

Figure 28: M_{ll}, njets, missing energy, $\triangle\phi_{lep12}$, leading and trailing lepton E_T. distributions in control region !Z with 1 tight + 1 loose leptons. Points are data and stacked histograms are background expectation.

the distributions for electron pairs, figure 38 for muon pairs.

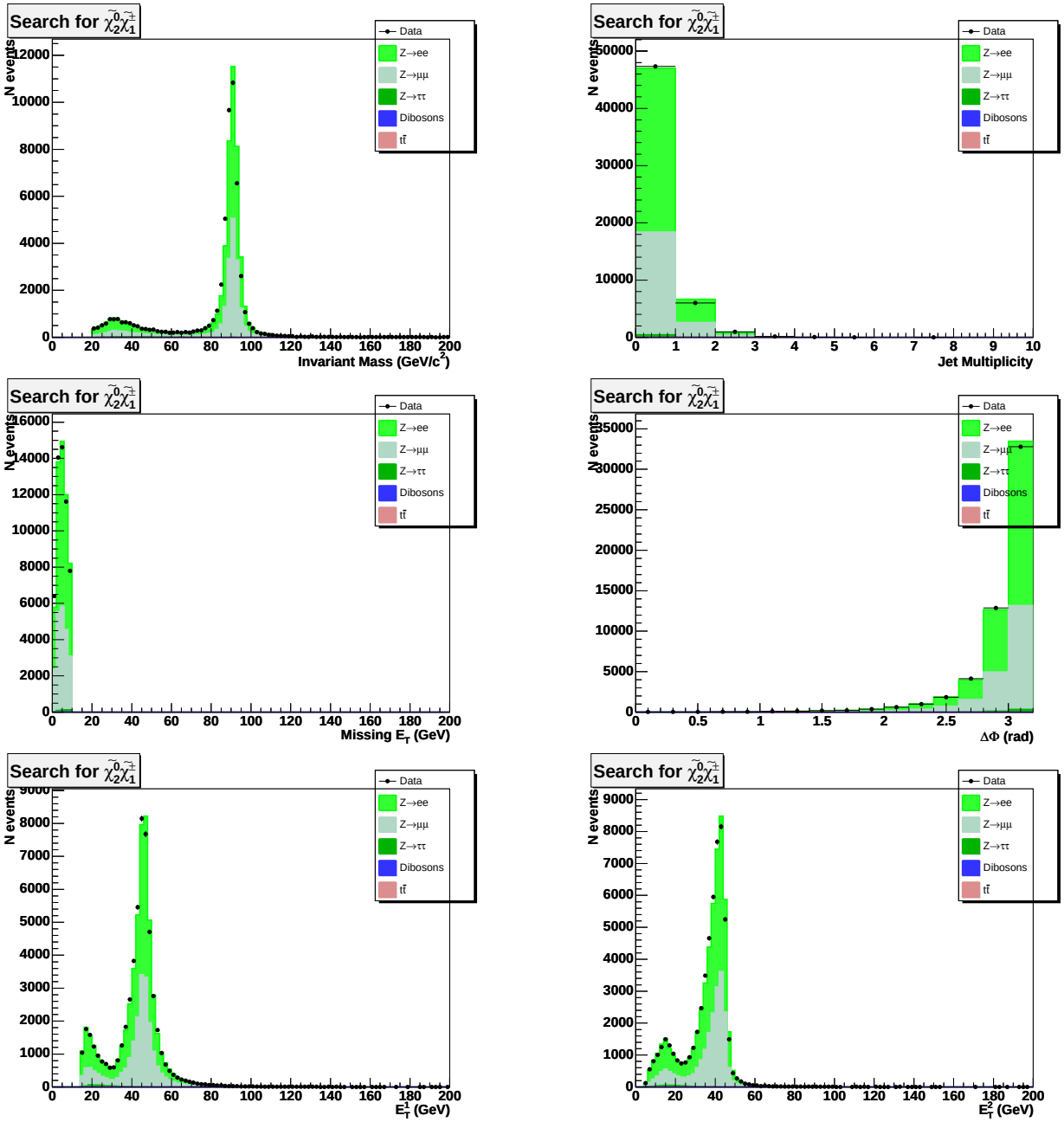

Figure 29: M_{ll}, njets, missing energy, $\triangle\phi_{lep12}$, leading and trailing lepton E_T. distributions in control region lo$\not{E}_T$ with 2 tight leptons. Points are data and stacked histograms are background expectation.

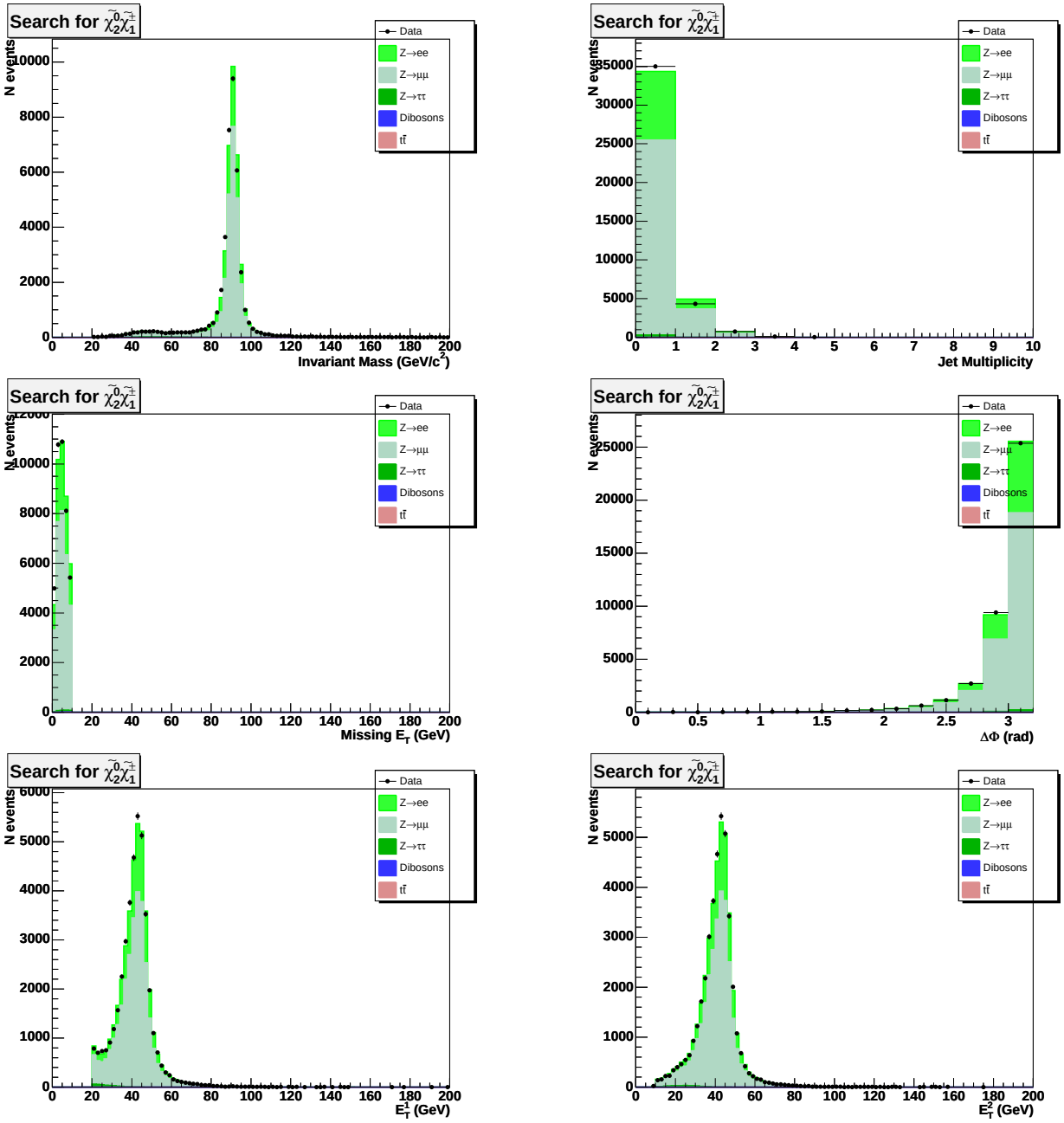

Figure 30: M_{ll}, njets, missing energy, $\triangle\phi_{lep12}$, leading and trailing lepton E_T. distributions in control region lo$\not{E}_T$ with 1 tight + 1 loose leptons. Points are data and stacked histograms are background expectation.

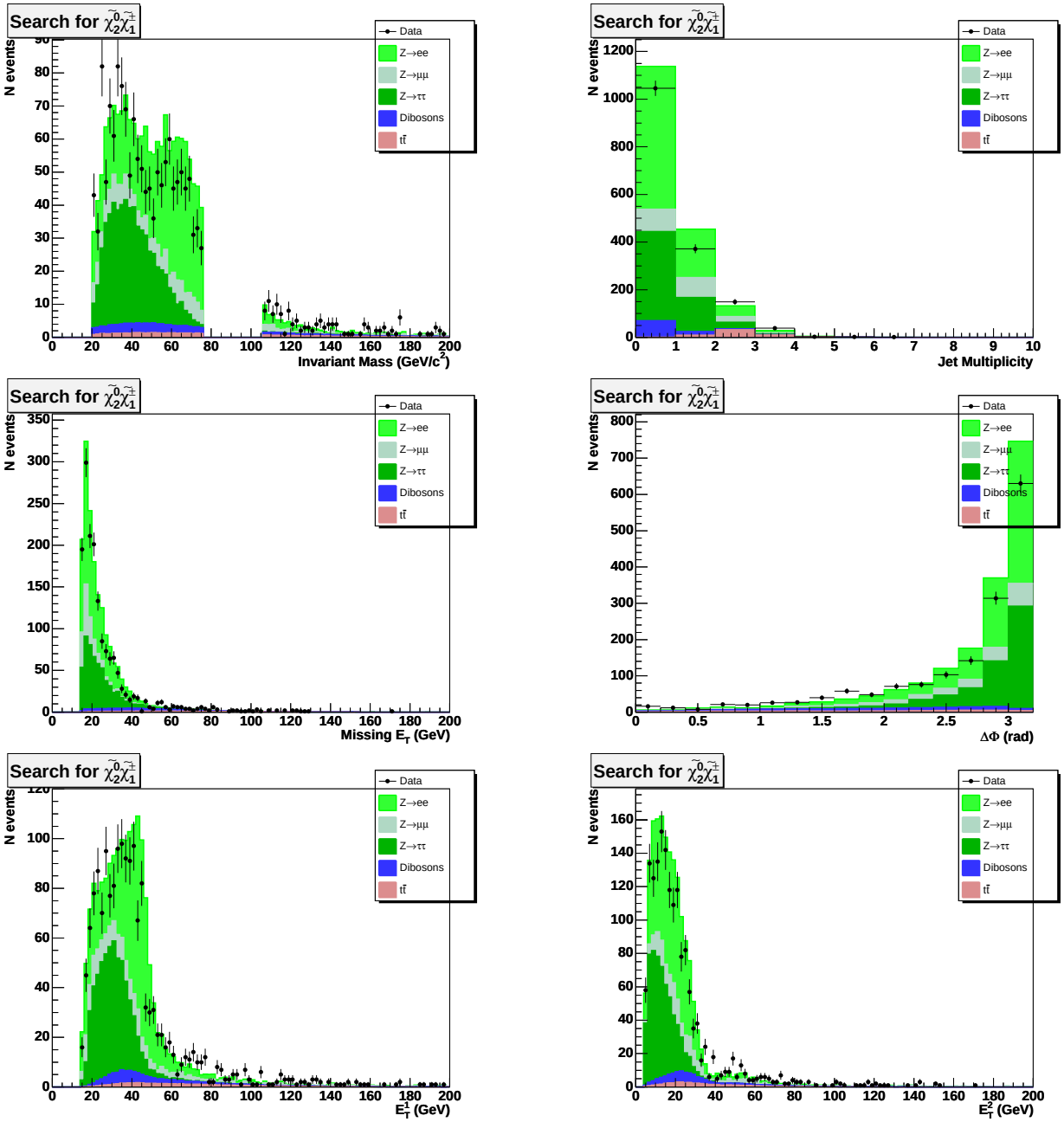

Figure 31: M_{ll}, njets, missing energy, $\triangle\phi_{lep12}$, leading and trailing lepton E_T. distributions in control region !Zhi with 2 tight leptons. Points are data and stacked histograms are background expectation.

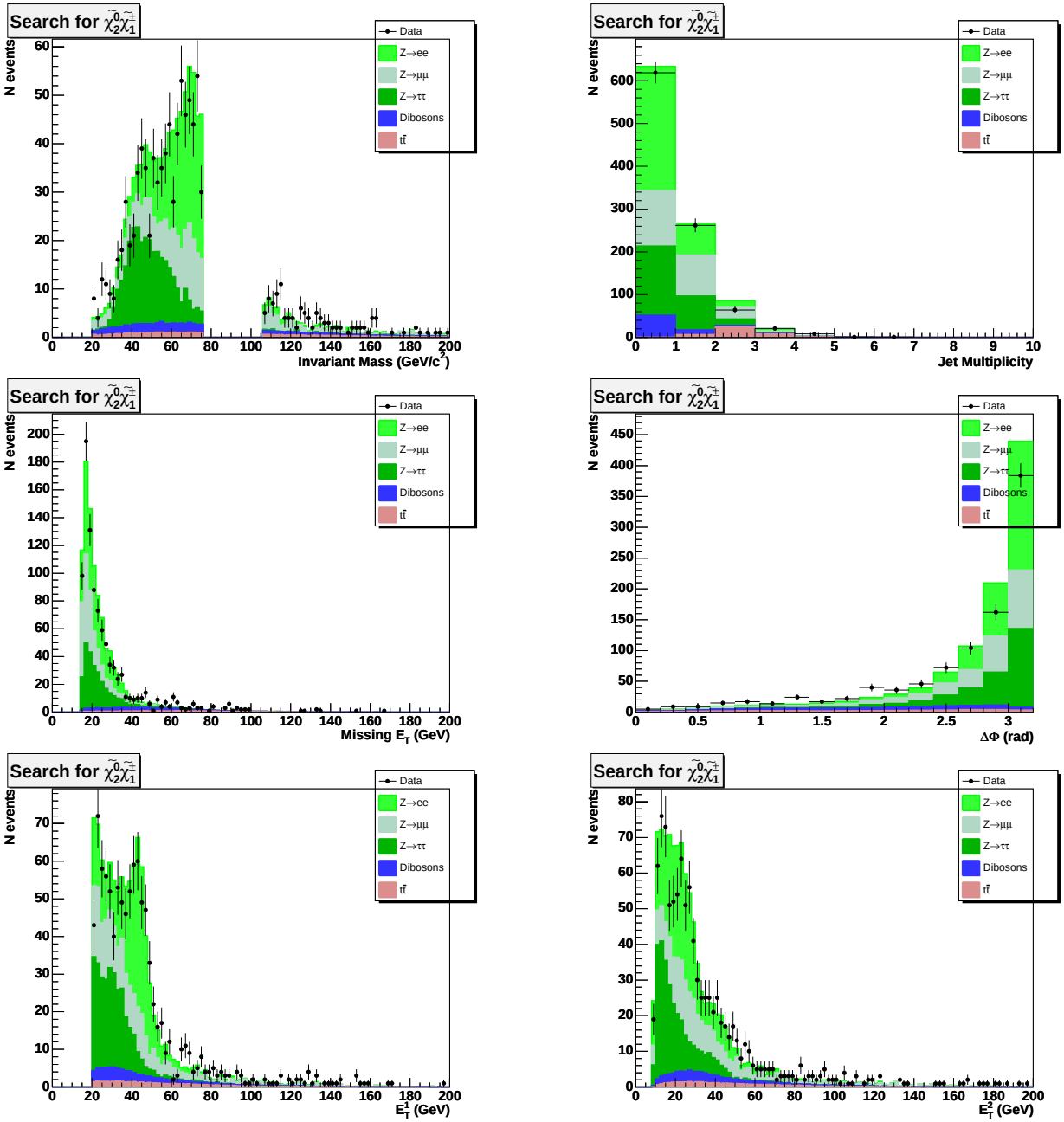

Figure 32: M_{ll}, njets, missing energy, $\triangle\phi_{lep12}$, leading and trailing lepton E_T. distributions in control region !Zhi with 1 tight + 1 loose leptons. Points are data and stacked histograms are background expectation.

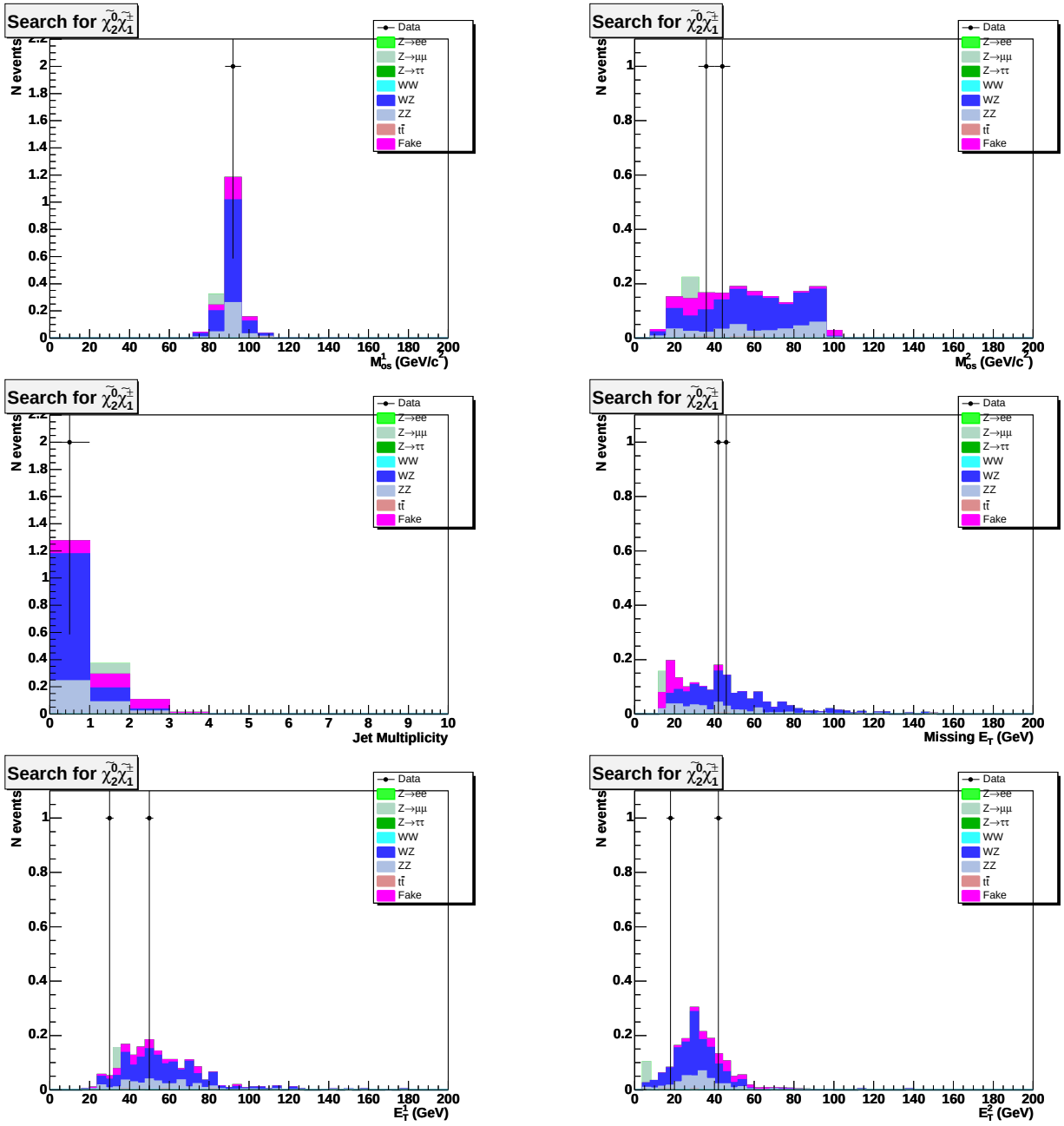

Figure 33: M_{os}^1, M_{os}^2, njets, missing energy, leading and next-to-leading lepton E_T distributions in control region Zhi with 2 tight leptons + 1 loose muon. Points are data and stacked histograms are background expectation.

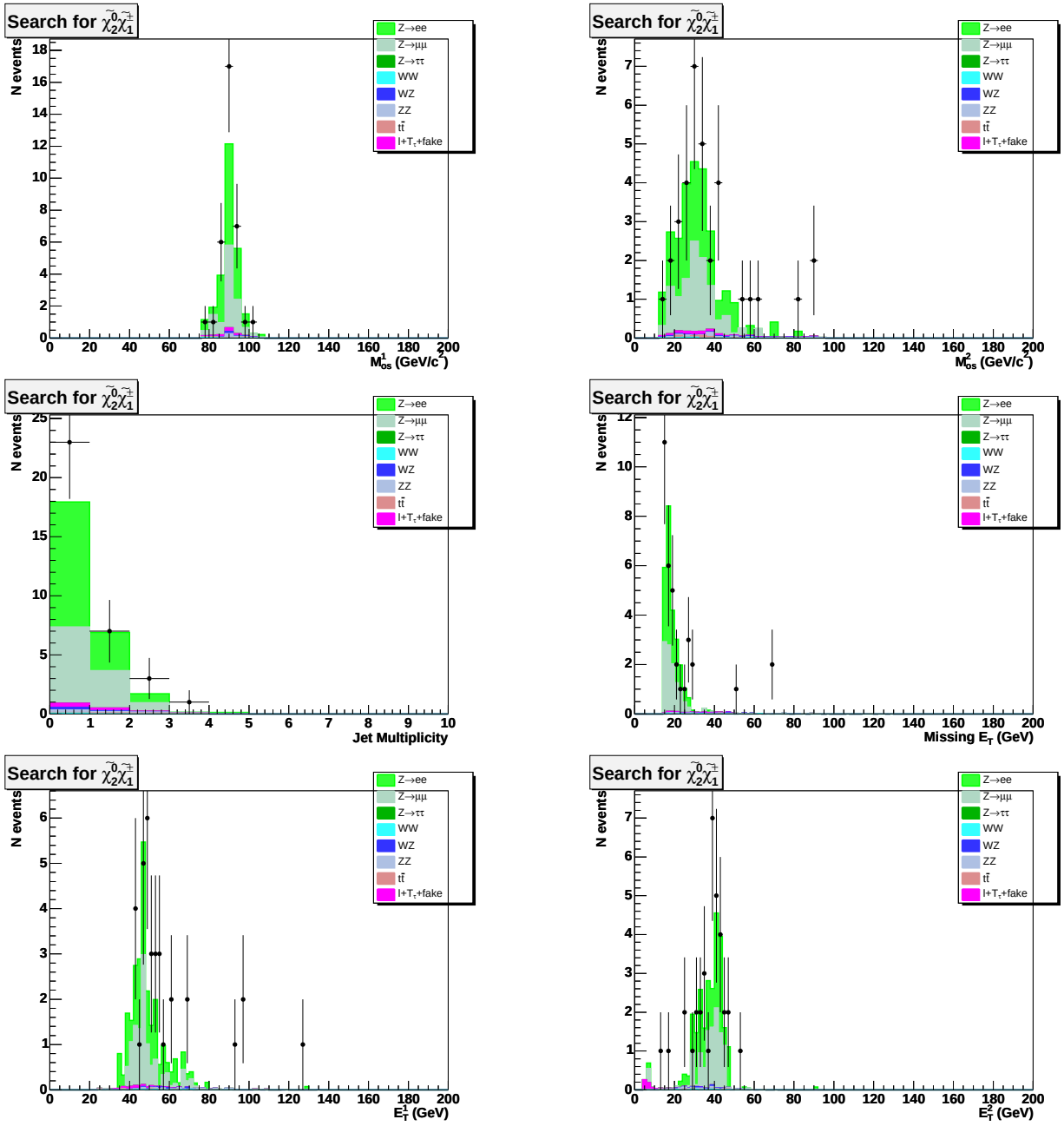

Figure 34: M_{os}^1, M_{os}^2, njets, missing energy, leading and next-to-leading lepton E_T distributions in control region Zhi with 2 tight lepton + 1 isolated track. Points are data and stacked histograms are background expectation.

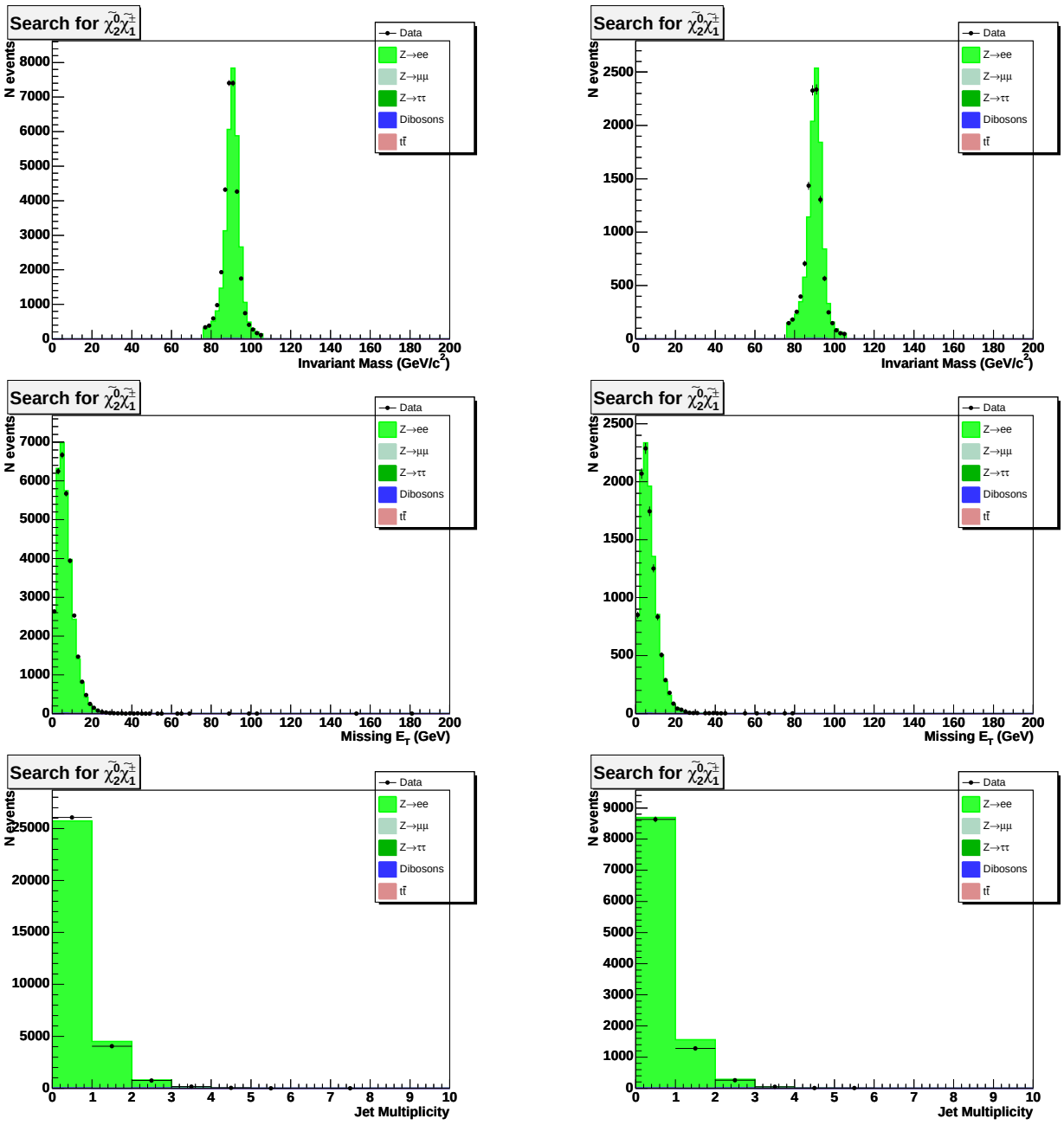

Figure 35: M_{os}^1, $\not\!\!E_T$, njets, distributions in control region Z with 2 tight electrons on left and 1 tight + 1 loose electron on right. Points are data and stacked histograms are background expectation.

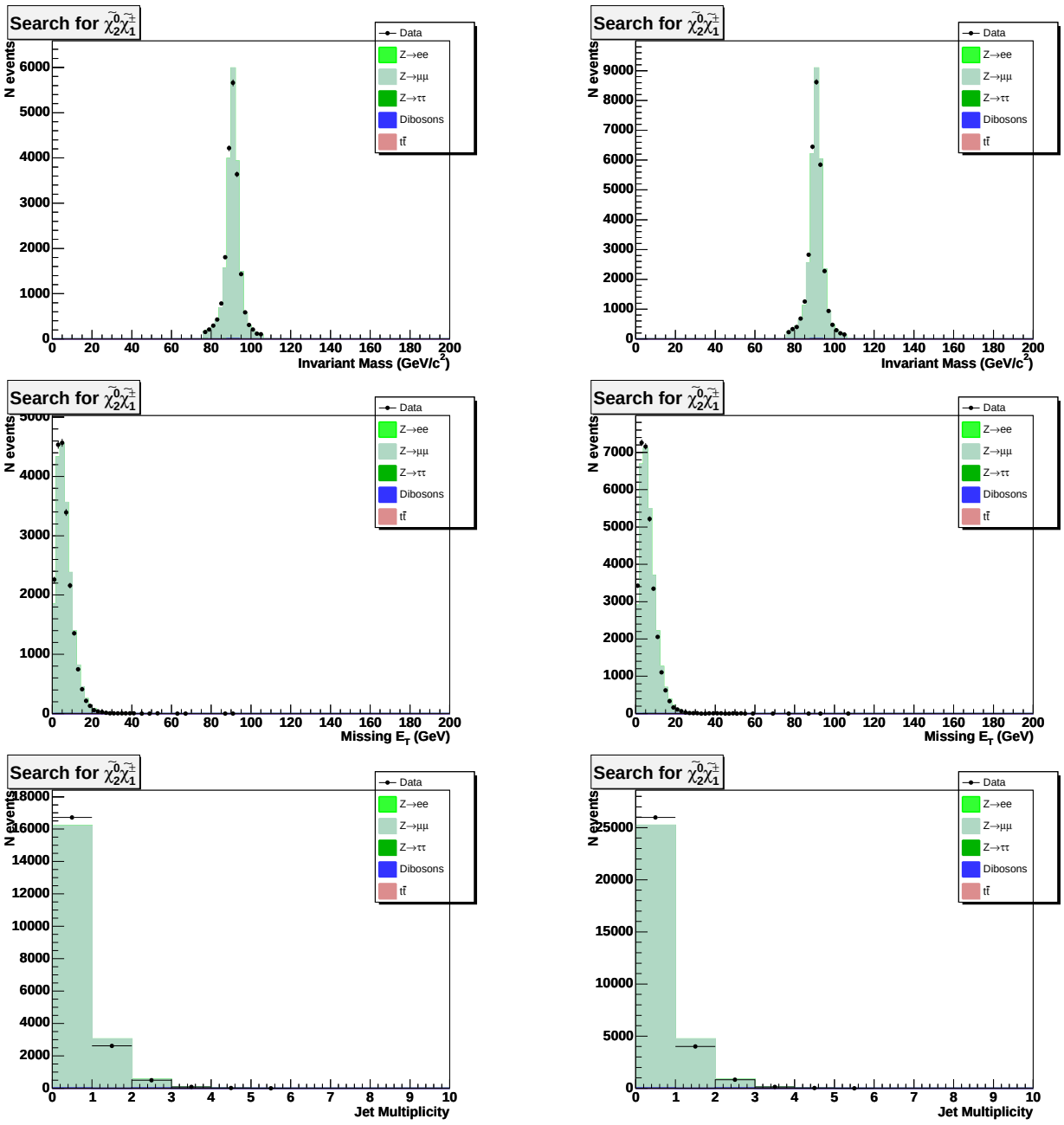

Figure 36: M^1_{os}, $\not\!\!E_T$, njets, distributions in control region Z with 2 tight muons on left and 1 tight + 1 loose muon on right. Points are data and stacked histograms are background expectation.

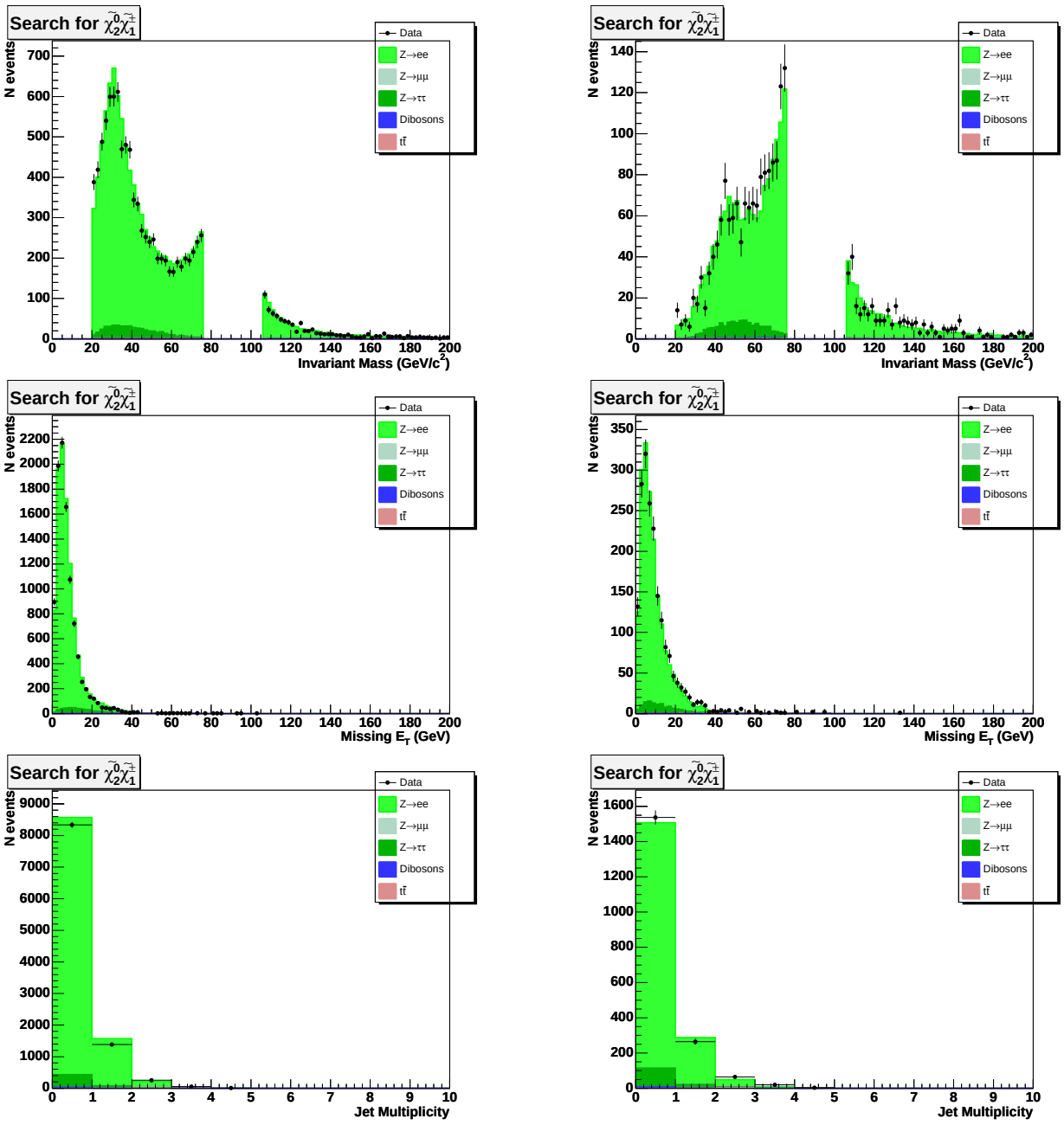

Figure 37: M_{os}^1, $\not\!\!E_T$, njets, distributions in control region !Z with 2 tight electrons on left and 1 tight + 1 loose electron on right. Points are data and stacked histograms are background expectation.

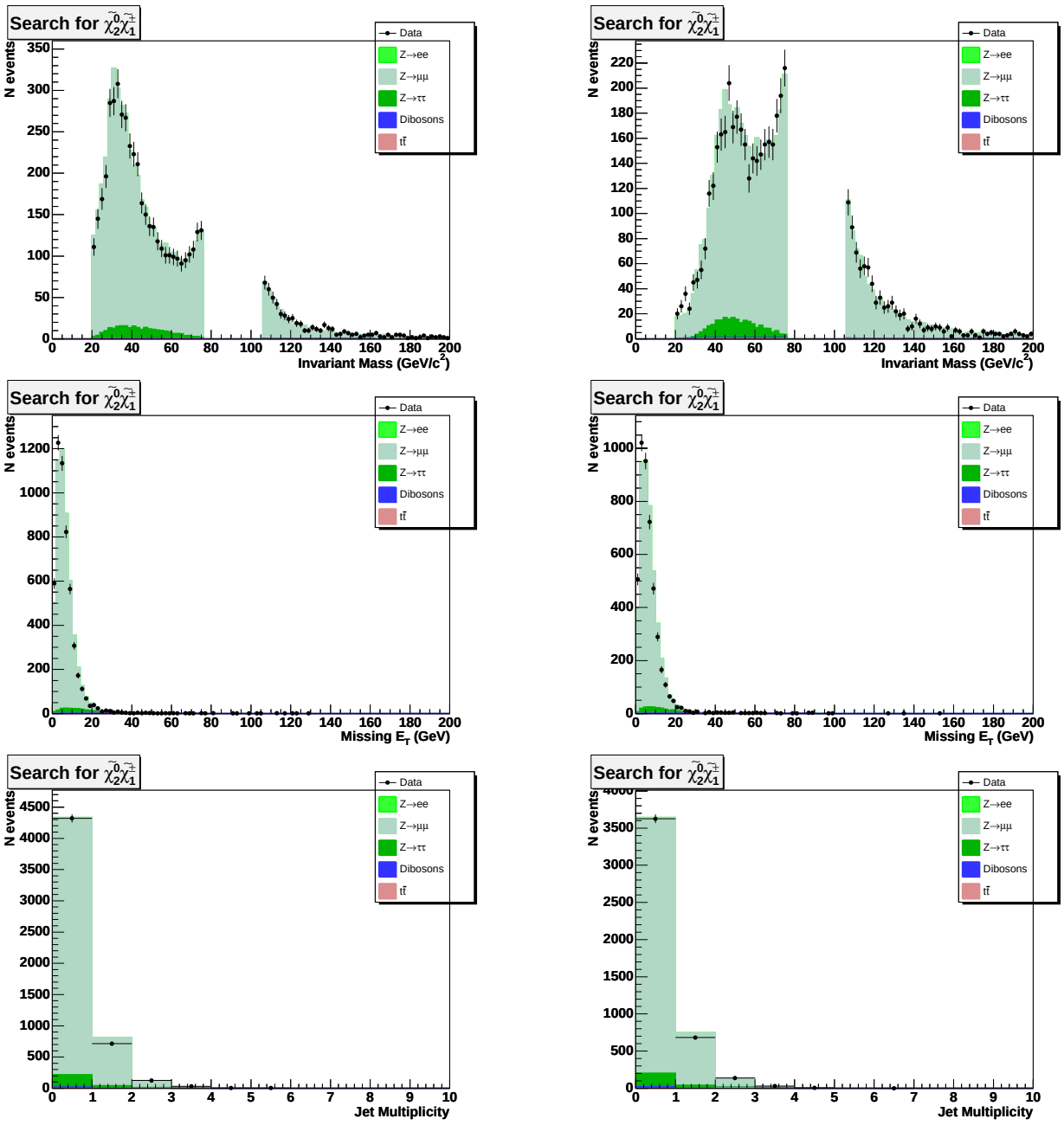

Figure 38: M^1_{os}, $\not\!\!E_T$, njets, distributions in control region !Z with 2 tight muons on left and 1 tight + 1 loose muon on right. Points are data and stacked histograms are background expectation.